# Inherent tracers for carbon capture and storage in sedimentary formations: composition and applications

# Inherent tracers for carbon capture and storage in sedimentary formations: composition and applications

**Stephanie Flude[1,2,*], Gareth Johnson[1], Stuart M. V. Gilfillan[1], R. Stuart Haszeldine[1]**

[1] School of Geosciences, The University of Edinburgh, Grant Institute, King's Buildings, James Hutton Road, EH9 3FE, UK. [2] Isotope Geosciences Unit, Scottish Universities Environmental Research Centre, Rankine Avenue, East Kilbride, G75 0QF, UK. * Corresponding author – sflude@gmail.com Tel: +44 (0)131 6507010 Fax: +44(0)131 6507340

## Abstract

Inherent tracers - the "natural" isotopic and trace gas composition of captured $CO_2$ streams – are potentially powerful tracers for use in CCS technology. This review outlines for the first time the expected carbon isotope and noble gas compositions of captured $CO_2$ streams from a range of feedstocks, $CO_2$-generating processes and carbon capture techniques. The C-isotope composition of captured $CO_2$ will be most strongly controlled by the feedstock, but significant isotope fractionation is possible during capture; noble gas concentrations will be controlled by the capture technique employed. Comparison with likely baseline data suggests that $CO_2$ generated from fossil fuel feedstocks will often have $\delta^{13}C$ distinguishable from storage reservoir $CO_2$. Noble gases in amine-captured $CO_2$ streams are likely to be low concentration, with isotopic ratios dependant on the feedstock, but $CO_2$ captured from oxyfuel plants may be strongly enriched in Kr and Xe which are potentially valuable subsurface tracers. $CO_2$ streams derived from fossil fuels will have noble gas isotope ratios reflecting a radiogenic component that will be difficult to distinguish in the storage reservoir, but inheritance of radiogenic components will provide an easily recognisable signature in the case of any unplanned migration into shallow aquifers or to the surface.

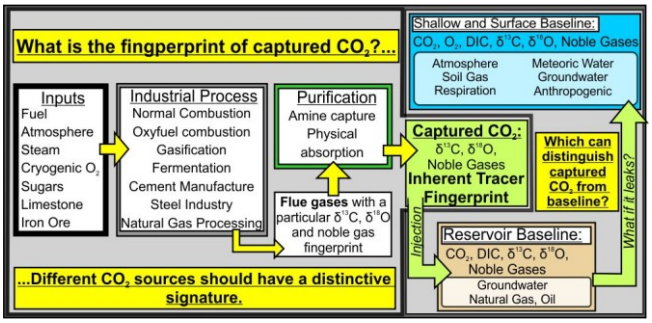


## 1. Introduction

### 1.1 The need for CCS

The link between atmospheric concentrations of anthropogenically produced $CO_2$ and global warming is unequivocal[1–4] and $CO_2$ emissions must be drastically reduced, and eventually stopped, if we are to avoid catastrophic, irreversible climate change. Carbon Capture and Storage (CCS) features prominently in all scenarios that consider timely and feasible reductions in $CO_2$ emissions[1,5]. Importantly, CCS is the only technology that can substantially reduce carbon emissions from industrial processes such as chemical synthesis and steel production. Climate models are increasingly relying on the use of negative emissions to limit global average temperature rise to 2 °C and include large amounts of bio-energy combined with CCS (BECCS), as this is the only feasible, industrial-scale negative emissions technology currently available[6].

Carbon capture in the context of this review involves removal of $CO_2$ from the flue gases of point-source emitters, such as power stations and industrial plants, to produce a stream of high concentration $CO_2$. Current well-developed capture techniques are often classified into one of three categories. (1) “Amine capture”, also referred to as “post combustion capture” because it was originally envisaged to be applied most often to fossil fuel or biomass combustion-fired power stations, removes $CO_2$ from a gas stream by chemical reaction of the $CO_2$ with an amine solvent (with or without the use of membranes), and is already widely used by the hydrocarbon industry to remove $CO_2$ from produced natural gas[7]. (2) “Oxycombustion” or “oxy-fuel combustion” produces a high $CO_2$ purity flue gas by burning fuel in an oxygen rich atmosphere, rather than air, and recycling the flue gas

into the combustion chamber. (3) “Pre-combustion capture” collects the $CO_2$ produced during gasification processes and is so named for the potential to generate hydrogen fuel, which can be combusted without producing $CO_2$ to produce electricity. These general carbon capture terms were developed in the context of CCS being most readily applied to electricity generation (hence the focus on pre- or post-combustion). In reality, these capture techniques are already applied to a much wider range of industrial activities, such as natural gas processing, Synfuel production and chemical / fertiliser manufacture (see Section 3), and so classification according to the stage of electricity generation is no longer appropriate. As such, we use the terms “amine capture”, “oxyfuel” and “gasification” when discussing these three different types of capture technique. Additional pressure-based adsorption techniques onto solid adsorbents (e.g. pressure-swing adsorption) or organic solvents are also used during gas purification, especially as part of the gasification processes.

The efficiency of $CO_2$ capture and the purity of the captured $CO_2$ stream vary between ~95% and 99.9%[2,8] depending on the capture method, post capture clean-up and specific conditions employed. Industrial specifications require a $CO_2$ purity of >95% for transport and storage, to maximise density and avoid problematic phase changes, and so end-product $CO_2$ streams tend to contain 90-99% $CO_2$, with minor to trace amounts of N=, hydrocarbons, $H_2S$, $NO_X$, $SO_X$, $O_2$, $H_2O$ and noble gases (especially Ar)[7–9].

**1.2 The need for $CO_2$ tracers**

Commercial scale carbon-storage projects will be required by governmental regulatory bodies to monitor $CO_2$ injected for storage and mitigate any unplanned behaviour, such as migration out of the storage reservoir (leakage) or to the surface (seepage), in the storage complex[10]. Furthermore, being able to trace the migration and reactions of injected $CO_2$ in the subsurface is fundamental to the continual assessment of injectivity, identification of $CO_2$ trapping mechanisms and quantification of storage capacity, all of which need to be well understood and characterised to ensure storage security.

Geophysical techniques, while useful monitoring tools, remain limited in their ability to quantify $CO_2$ pore space saturation and dissolution at high spatial resolution[11–13]. Seepage rates of 0.001 - 0.01% per year are generally considered acceptable on a climate accounting basis, amounting to a loss of ~1% of the injected $CO_2$ over 100 years, a target adopted by the U.S. Department of Energy[14,15]. Conclusive detection of such seepage rates by measurement of $CO_2$ concentrations remains problematic due to natural background $CO_2$ fluctuations. A potential solution to this problem is the use of geochemical tracers, detectable at low concentrations due to their low background level in the atmosphere or storage complex. Addition of geochemical tracers for environmental monitoring and interpretation of reservoir dynamics is a long-standing practice in the hydrocarbon industry, with perfluorocarbon tracer compounds (PFTs)[16], tritiated and perdeuterated $CH_4$ and $H_2O$, freons, sulphur hexafluoride ($SF_6$)[17] and noble gases such as Kr and Xe[18] proving to be particularly useful tracers.

Tracers can be classified in terms of their relationship to the injected $CO_2$ as 1) added tracers (substances added to the $CO_2$ stream prior to injection, e.g. $SF_6$), 2) inherent or natural tracers (substances already present in the $CO_2$ stream or the isotopic composition of the $CO_2$ itself), or 3) indirect tracers (changes to baseline values resulting from interaction of the $CO_2$ with the natural environment, e.g. pH or cation content due to mineral dissolution)[19]. Adding geochemical tracers to injected $CO_2$ can facilitate detailed monitoring and modelling of $CO_2$ storage, but concerns remain regarding the economic cost of tracers in commercial scale storage sites, the possibility of increased background (lower sensitivity) / site contamination, and the environmental impact of such compounds[17,20–22]. PFTs and $SF_6$, in particular, are potent greenhouse gases with atmospheric residence times of 1000s of years[17,22].

Using the isotopic and trace element geochemistry of the injected $CO_2$ itself as a tracer has the potential to facilitate in-reservoir tracing and leakage monitoring with minimal economic and environmental impact compared with added tracers. Furthermore, Article 12.1 of the EU directive on

CCS states that "no waste or other matter may be added for the purpose of disposing of [the $CO_2$]"[10]; while provision has been made in the directive for allowing the addition of tracers, these require consideration on a case-by-case basis and so use of inherent $CO_2$ tracers may help to simplify applications for $CO_2$ storage permits.

Here, we describe the inherent tracers which will be most useful for fingerprinting and monitoring $CO_2$ during storage, summarise the currently available information regarding inherent tracer signatures in both captured $CO_2$ and potential storage reservoirs, and highlight the further research necessary to facilitate the application of inherent tracer geochemistry to CCS. As we will show, the feasibility of using inherent tracers for measuring, monitoring and verification (MMV) depends on a number of variables, including the baseline composition of reservoirs and overburden of interest and the inherent tracer composition of the captured $CO_2$ stream. These will vary extensively depending on a number of factors and hence specific discussion of detection limits of the inherent tracers we describe is out of the scope of this review.

## 2. Inherent Tracers

For tracers to be effective, their compositions must be distinct from that of the storage site, including the host reservoir, overburden and local atmosphere. In this section we provide a brief background to and highlight further information on the isotope and trace gas systems that may be used as inherent tracers.

### 2.1 $CO_2$ Isotopic composition

The stable isotopes of C and O of injected $CO_2$ are an obvious potential tracer and have been successfully used in a number of projects to identify $CO_2$ migration and quantify pore space saturation and dissolution of $CO_2$ (see Section 6). Much of this work and background theory relevant to CCS has recently been summarised in a number of review papers[12,19,23–26]. However, the isotopic composition

of the captured $CO_2$ itself, has received less attention, which we address in Section 3. For this review, we concentrate on using C-isotopes as a means of fingerprinting the injected $CO_2$. While O-isotopes of captured $CO_2$ may be a useful, quantitative monitoring tool[11], rapid equilibration of O-isotopes between $CO_2$ and water[27] means that the O-isotope composition of $CO_2$ will be controlled by any volumentrically significant water it interacts with; as a result, the O-isotope composition of $CO_2$ is expected to change significantly after injection into the storage reservoir and so not provide a diagnostic tracer of the $CO_2$ itself. Hence O-isotopes are not discussed in detail in this review.

For context, the range of isotopic compositions occuring in nature are shown in Figure 1 with details provided in Supplementary Data Table S1. C-isotope values are presented in $\delta^{13}C$ relative to Vienna Pee Dee Belemnite (V-PDB), where

$$\delta^{13}C\ ‰ = \left(\frac{(^{13}C/^{12}C)_{sample}}{(^{13}C/^{12}C)_{reference}} - 1\right) \times 1000$$

Isotope fractionation, enrichment factors (Ɛ), and conversion between isotopic values relative to different standards are covered in detail in recent review papers which we refer interested readers to[12,19,23–26].

### 2.2 Noble gases

Noble gases (He, Ne, Ar, Kr, Xe) are particularly useful for tracing interaction of gases with fluids due to their unreactive nature and Henry's Law controlled solubility; in general, solubility increases with elemental mass and decreases with increasing temperature. Noble gases will preferentially partition into gas > oil > fresh water> saline water, and so mixing and migration of different fluids and gases in the subsurface may lead to multiple re-equilibration events that result in elemental fractionation of the noble gases[28,29]. Hence, noble gases are being increasingly used to identify and quantify hydrocarbon migration pathways from modelling the elemental fractionation that occurs during partitioning between water, oil and gas[30,31]. Noble gases in the subsurface can be considered a mixture

of three components[32]: 1) Atmospheric derived noble gases, introduced to the subsurface by equilibration with meteoric water and recharge; 2) radiogenic noble gases produced in situ by decay of radioactive elements; 3) terrigenic fluids originating from defined geochemical reservoirs. Two common terrigenic components in sedimentary formations are crust and mantle. Mantle noble gases are enriched in $^{3}He$, with $^{3}He/^{4}He$ as high as 70 $R_A$ ($R_A$ being $^{3}He/^{4}He$ of atmosphere, $1.339 \times 10^{-6}$) while crustal noble gases are enriched in radiogenic noble gases ($^{4}He$ and $^{40}Ar$) and have $^{3}He/^{4}He$ <0.7 $R_A$[32]. In subsurface fluids a distinction exists between radiogenic and crustal components; the terrigenic crustal component is derived from radioactive decay, but represents the cumulative accumulation in the host rock, and is thus controlled by the age and chemistry of the geological formation hosting the fluid and the openness of the system, while the radiogenic component is added to the fluid by in situ-radioactive decay and is thus a function of the host formation chemistry and fluid residence time[32]. Summaries of noble gas data relevant to CCS are shown in Table 1.

## 3. Geochemistry of the captured $CO_2$ stream

Two sources of information are available to assess the likely composition of the captured $CO_2$ stream: 1) a limited number of direct measurements on captured $CO_2$, and 2) hypothetical considerations of the feedstocks and processes involved in $CO_2$ generation. We analyse this information to draw conclusions about the range of $CO_2$ compositions that can be expected for different feedstocks and processes, which are summarised in Table 2. Further information regarding $\delta^{13}C$ and noble gas content of a range of relevant feedstocks are provided in the Supplementary Information.

### 3.1 Direct measurement of the captured $CO_2$ stream.

CCS projects have reported captured $CO_2$ stream data from two oxy-combustion plants, three Synfuel / hydrogen production plants, two fertiliser manufacturers, one natural gas processing plant and one unknown combustion source. $\delta^{13}C$ has been the most widely analysed tracer in captured $CO_2$ to date, giving a wide range of values from -51 to -4.7 ‰. Limited noble gas data is available for $CO_2$ streams

from fertiliser and oxyfuel plants. The limited available data is consistent with theoretical considerations discussed below, but the uncertainties involved (most often relating to the precise feedstock composition) hinder robust predictions of captured $CO_2$ stream chemistry and more studies are needed to clarify the $\delta^{13}C$ of captured $CO_2$.

### 3.2 Fuel combustion for energy production

Power stations are some of the largest point-sources of $CO_2$ emissions in the developed world making them obvious targets for CCS. In most cases, power is generated by combustion of material, often fossil fuels but with an increasing use of biomass, to drive a turbine and generate electricity. Capture of combustion-produced $CO_2$ will be either via amine capture or oxyfuel methods.

#### *3.2.1 Carbon isotopes:*

For $CO_2$ derived from fossil fuel combustion, Widory[33] identified $^{13}C$ depletion in the $CO_2$ relative to the fuel, amounting to $\delta^{13}C$ ~ -1.3 ‰ for a range of fossil fuel types (solid, liquid, gas). More recent work has measured $\delta^{13}C$ during coal combustion and found that resulting $CO_2$ has $\delta^{13}C$ between -2.39 and +2.33 ‰ relative to the coal feedstock[34]. $\delta^{13}C_{CO_2}$ of -46.2 ‰[35] has been reported for $CO_2$ derived from combustion of natural gas, which is consistent with (the admittedly wide range of) expected values (Figure 1) but the capture method was not reported.

For biomass, complete combustion of C3 and C4 plants produces $CO_2$ with the same C-isotope composition of the bulk plant, but partial combustion of C4 plants may result in $^{13}C$ enrichment of the $CO_2$ (up to +4 ‰ at 3% combustion)[36]. The C-isotope signature of $CO_2$ produced by burning biomass will therefore depend on the specific feedstock and the efficiency of the combustion process. Given the higher temperatures associated with oxy-combustion, we might expect a higher efficiency of biomass combustion compared to normal combustion and so no isotopic fractionation would be expected. Reported $\delta^{13}C$ of $CO_2$ from oxy-combustion of natural gas (-40 ‰, Rousse CCS Project[37]) and

lignite (-26 ‰, Ketzin CCS project, see supplementary Table S2) are consistent with expected values (-61 to -21.3 ‰ and -31.3 to -21.3 ‰, respectively -Table 2).

***3.2.2 Noble gases:***

To the best of our knowledge, very little data is available on the noble gas content of combustion gases. Noble gases in combustion flue gases will be derived from the material being combusted and from the combustion atmosphere (air for normal combustion, cryogenic oxygen for oxyfuel). Concentrations of most noble gases in hydrocarbons are generally two to three orders of magnitude lower than in air (Table 1) and so atmospheric noble gases are expected to dominate. A radiogenic or terrigenic isotopic component might be resolvable in hydrocarbon-derived $CO_2$ due to elevated $^{4}He$ in fossil fuels.

For oxyfuel, additional heavy noble gases (Ar, Kr, Xe) may be introduced with the cryogenically purified $O_2$. $CO_2$ injected at the Rousse CCS project was derived from oxy-combustion of natural gas[37]. The source natural gas fuel was enriched in $^{4}He$ and depleted in $^{20}Ne$, $^{36}Ar$, $^{40}Ar$, and $^{84}Kr$ relative to air[37]; the resulting $CO_2$ remained enriched in $^{4}He$ and depleted in $^{20}Ne$ relative to air, but Ar isotopes had concentrations similar to air and $^{84}Kr$ was enriched by an order of magnitude compared to air[37]. Enrichments of Ar (up to 2%) in oxyfuel captured $CO_2$ have also been observed during oxyfuel pilot experiments[8], despite distillation procedures designed to remove inert gases[7].

**3.3 Gasification processes / Synfuel production / Pre-combustion $CO_2$ capture.**

Here we use the term “gasification processes” to refer to the range of reactions used to generate Syngas ($H_2$ and CO) from a variety of fuel stocks. Syngas can be further processed by Fischer-Tropsch reactions to create a range of chemicals and synthetic fuels (Synfuels), including synthetic natural gas (SNG) and Fisher-Tropsch liquid fuels. These chemical reactions are described in the supplementary information.

Syngas is generated by a two stage chemical reaction. At the first stage, carbon monoxide (CO) and $H_2$ are produced from the feedstock, via either steam reforming or partial oxidation, followed by addition of steam to stimulate a "shift reaction" that converts CO to $CO_2$, generating more $H_2$[7]. For synfuel production the syngas stream is passed through a synthesis reactor where CO and $H_2$ are catalytically converted to the desired chemical[7]. $CO_2$ from the entire process is captured both upstream and downstream of the synthesis reactor and the captured $CO_2$ will be a combination of $CO_2$ generated from different gasification stages, with a decreased input from the shift reaction as CO is used in Fischer-Tropsch reactions. The resulting $CO_2$ is removed from the gas stream by either chemical solvents (e.g. amine capture) or physical solvents (e.g. cold methanol)[7].

***3.3.1 Carbon-isotopes:***

Fractionation of C-isotopes during gasification is likely due to increased bond strength of $^{13}C$-$^{12}C$ compared to $^{12}C$-$^{12}C$, resulting in $^{13}C$ depletion in low molecular weight gases and $^{13}C$ enrichment in heavy residues like tar and vacuum bottoms[38]. C-isotope ratios will be $\delta^{13}C_{CO} < \delta^{13}C_{CH4} < \delta^{13}C_{hydrocarbons} < \delta^{13}C_{coal} < \delta^{13}C_{char} < \delta^{13}C_{CO_2}$ at typical gasification temperatures (> 1000°C)[39–41] . This suggests that any $CO_2$ produced by incomplete reactions in the first stage of gasification is likely to be enriched in $^{13}C$ compared to the original feedstock, while the resulting CO will be depleted in $^{13}C$. This agrees with experimental results from underground coal gasification plants[38,40,42], and natural gas generation via pyrolysis of coal and lignite[43,44], which produced $CO_2$ enriched in $^{13}C$ by 2-10 ‰ relative to the feedstock. Conversely, $CO_2$ generated from CO via the shift reaction will be depleted in $^{13}C$. In a simplistic scenario, all $CO_2$ resulting from gasification will be derived from the shift reaction and so we could expect $CO_2$ captured from Syngas plants to be the same as or isotopically lighter than the feedstock, depending on the efficiency of the gasification reactions and proportion of feedstock not converted to Syngas. For synfuel and F-T plants, the $^{13}C$ depleted CO will be used in chemical synthesis and so early-generated, $CO_2$ slightly enriched in $^{13}C$ will dominate. In reality, gasification of solid fuels

is likely to produce $CO_2$ and $CH_4$ in addition to CO and $H_2$, and so the isotopic composition of resulting $CO_2$ will depend on the proportions of $^{13}C$-enriched, early-produced $CO_2$ and $^{13}C$-depleted, shift-reaction $CO_2$. It is thus difficult to precisely predict the C-isotopic composition of $CO_2$ captured from syngas and synfuel plants. However, it is likely that the various fractionation and mixing processes will average out, giving $CO_2$ with an isotopic composition similar to, or slightly more $^{13}C$-depleted than the feedstock for syngas plants, and similar to or slightly more $^{13}C$-enriched than the feedstock for chemical and synfuel plants.

One of the sources of $CO_2$ injected at the Ketzin project was reportedly a by-product of hydrogen production[45] at an oil refinery[46]. This $CO_2$ has $\delta^{13}C$ ~-30.5 ‰[46] (Table S2) which is indistinguishable from the range of $\delta^{13}C$ values expected for oil (-18 to -36 ‰, Table 2). $CO_2$ injected in the Frio project was derived from a refinery in Bay City, Texas, and the Donaldsonville fertiliser plant, Louisiana[47]. Reported $\delta^{13}C$ of the injected $CO_2$ was -51 to -35 ‰[48]. While the end-member $\delta^{13}C$ compositions were not reported, the values are consistent with those for natural gas (fertiliser plant) and oil (refinery) (see Table 2 and Figure 1). $CO_2$ captured from the Scotford Bitumen Upgrader, Canada, was derived from hydrogen production and purified using amine capture[49]; most hydrogen production in the region is produced using steam methane reforming[50]. The captured $CO_2$ has $\delta^{13}C$ of -37 ‰[51], which is within the range of $\delta^{13}C$ values for natural gas. While the range of possible feedstock compositions is too wide to be conclusive, this data is consistent with our above predictions. The $CO_2$ injected at Weyburn is generated via coal gasification at the Great Plains Synfuel Plant, North Dakota, USA, and has a $\delta^{13}C$ of -20 to -21 ‰[52]. This is indistinguishable from the (wide) range of $\delta^{13}C$ for coal of -30 to -20 ‰ (Table 2). Data are not available for the coal and lignite used in the Synfuel plant, but coals and lignite from North Dakota have $\delta^{13}C$ between -25 and -23 ‰ with a minority of coal beds reaching -20 ‰[53]. The captured $CO_2$ from the Synfuel plant is thus at the $^{13}C$-enriched end of the range of likely feedstock isotope values, consistent with our prior discussion.

279

280 ***3.3.2 Noble gases:***

281 The noble gas composition of the captured $CO_2$ stream generated by gasification processes is likely to
282 be controlled by the noble gas content of the feedstock and the steam and oxygen used in the
283 gasification processes. Steam is likely to introduce noble gases that are a mixture of atmosphere and
284 air saturated water (ASW) for the source water. Gasifiers that use partial oxidation rather than steam
285 reforming will likely produce $CO_2$ enriched in heavy noble gases (Ar, Kr, Xe) from added $O_2$.

286

287 **3.4 Fermentation**

288 Fermentation of biomass to produce ethanol as a sustainable fuel source is a well-developed industry
289 in the USA and Brazil; while the total anthropogenic $CO_2$ emissions from bioethanol fermentation
290 make up less than 1% of global $CO_2$ emissions, the $CO_2$ gas stream is of high purity and so a suitable
291 target for early adoption of CCS[7]. The two main crops used for bioethanol production are currently
292 corn / maize (USA) and sugarcane (Brazil), both of which are C4 photosynthetic pathway plants[54].
293 Various other C4 crops, such as miscanthus switchgrass, and C3 plants such as poplar[55] are under
294 investigation as suitable bioethanol feedstocks due to the their ability to grow in relatively arid
295 climates and their lack of economic competition as a food crop[54]. Ethanol is produced from the
296 feedstock by fermentation of the sugars and starches in the biomass, generating a pure stream of $CO_2$
297 via:

298 $C_6H_{12}O_6 \rightarrow 2C_2H_5OH + 2CO_2$ [reaction 1][56]

299

300 ***3.4.1 Carbon-isotopes:***

301 The carbon isotopic composition of plant sugars generally reflects the bulk plant composition; $\delta^{13}C$ of
302 glucose from sugar beet (C3) is ~-25.1 ‰[57] (c.f. -30 to -24 ‰, Table 2) and from maize (C4) is $\delta^{13}C$ ~-
303 10.5 ‰[57] (c.f. -15 to -10‰, Table 2). Carbon isotopes are not evenly distributed within the glucose
304 molecules and this results in fractionation of C-isotopes during fermentation[57,58]; the 3rd and 4th carbon

atoms in the glucose chain are enriched in $^{13}C$ relative to the bulk sugar, and these form the resulting $CO_2$[58]. Different degrees of $^{13}C$ enrichment of 3rd and 4th position C-atoms occur between C3 and C4 photosynthetic pathway plants, resulting in hypothetical $^{13}C$ enrichment of fermentation-produced $CO_2$ over glucose of ~+8.2 ‰ for C3 plants and +4.5 ‰ for C4 plants[58]. Measured $CO_2$-glucose isotope fractionation factors range from +7.4 to +4.6 ‰ for C3 plants and +5.1 ‰ for C4 plants[58–60]. Apples are C3 plants and $CO_2$ produced during fermentation of cider has been measured with $\delta^{13}C$ of -25 to -21 ‰, which is enriched by at least 3 ‰ relative to C3 plants[61].

Assuming that bioethanol feedstock will be dominated by C4 biomass, and that $CO_2$ produced by fermentation is enriched in $^{13}C$ by 4 to 6 ‰ relative to the original sugars, we can expect $CO_2$ captured from fermentation plants to have $\delta^{13}C$ of ~-11 to -4 ‰.

***3.4.2 Noble gases:***

The main source of noble gases during fermentation will be air saturated water (ASW) in the fermenting solution. Noble gases are more soluble in organic solvents, so we would expect solubility to increase as fermentation proceeds, resulting in noble gas depletion in the $CO_2$ stream.

**3.5 Cement Industry**

Cement production (including energy to drive the process and indirect emissions) contributes ~6% of global anthropogenic $CO_2$ emissions, ~50% of which is from calcination of limestone to produce lime and $CO_2$:

$$CaCO_{3(s)} \rightarrow CaO_{(s)} + CO_{2(g)} \qquad \text{[reaction 2]}[62,63].$$

The remaining emissions are from the energy required to fire the kiln; coal is commonly used but other fuels, such as natural gas, may be used. Likely carbon capture solutions for the cement industry include oxyfuel combustion to heat the kiln or amine capture for both kiln combustion and calcination gases[62].

### *3.5.1 Carbon-isotopes:*

Calcination reactions are assumed to not cause isotopic fractionation, so the resulting $CO_2$ has the same isotopic composition as the initial carbonate[64,65] – i.e. $\delta^{13}C \sim 0$. Assuming a 50:50 mixture of $CO_2$ derived from calcination and from coal combustion we would expect $CO_2$ emitted from cement factories to have $\delta^{13}C$ between ~-11 and-16 ‰.

### *3.5.2 Noble gases:*

As the noble gas content of limestone is low (see supplementary information S.1.5), calcination of limestone is unlikely to significantly contribute noble gases to the $CO_2$ stream, which will be dominated by noble gases from fossil fuel combustion from firing the kiln.

## 3.6 Iron and Steel Industry

The steel industry generates 1.9 tonnes of $CO_2$ per tonne of steel[66] contributing 4 to 7% of global anthropogenic $CO_2$ emissions. $CO_2$ is generated from two processes: energy for steel production by burning of fuel and the use of reducing agents for steel production from iron ore, the most readily available reducing agent being coal[66]. Integrated steel plants (ISP) use mostly coal, with minor natural gas and oil, as both the fuel and reducing agent, while mini-mill plants use electric furnaces to heat and melt scrap or direct-reduced iron (DRI)[7]; while mini-mill plants may not directly produce $CO_2$ emissions, DRI is produced by reacting iron ore with $H_2$ and CO to form iron + $H_2O$ + $CO_2$[7].

### *3.6.1 Carbon isotopes:*

According to our investigations, there is no published data for carbon isotope fractionation between steel and $CO_2$, hence estimating $\delta^{13}C$ of $CO_2$ produced by integrated steel plants is difficult, but likely to be dominated by combustion $CO_2$ (so $\delta^{13}C$ of -31 to -21 ‰). In the case of DRI production an obvious source of $H_2$ and CO for the reduction process is Syngas. In this case, the $\delta^{13}C$ of $CO_2$ resulting from

iron reduction would likely mirror that of the CO, as discussed for Syngas production (i.e. slightly depleted in $^{13}C$ relative to the gasification feedstock -Section 3.3).

### *3.6.2 Noble gases:*

The overall noble gas budget of $CO_2$ emitted from steel plants will be dominated by atmospheric noble gases incorporated during combustion, for integrated steel plants, and noble gases introduced during syngas production for mini-mill plants. However, given the low concentration of He in air, enrichment of iron-ore derived radiogenic $^{4}He$ may be significant.

## 3.7 $CO_2$ separation

### *3.7.1 Chemical absorption*

Chemical absorption involves passing flue gases through a solvent with a high affinity for $CO_2$ (most commonly an amine solvent). In a typical amine capture process a $CO_2$-bearing flue gas is reacted with the amine solvent at ~ 40 to 60 °C and the remaining flue gas (which will contain some residual $CO_2$) cleaned and vented; the $CO_2$-bearing solvent is transferred to a desorber vessel and heated to 100-140 °C to reverse the $CO_2$-binding chemical reaction and release a stream of pure (>99%) $CO_2$ gas[7,67]. Typical $CO_2$ recoveries are 80% to 95% of the $CO_2$ in the flue gas[7]. Such techniques are commonly employed to remove $CO_2$ from natural gas, before it is piped to national gas grids[7]. Various capture plants and aqueous amine solvents are being developed for chemical absorption of $CO_2$. The effects on inherent tracer composition will likely depend on the relative efficiencies of the absorption / desorption processes used by the capture process, the specific chemical reaction pathways that occur and the temperature and pH of the reactions. Two reaction pathways are common for amine solvents: bicarbonate ($HCO_3^-$) and carbamate ($NH_2CO_2^-$) formation[67].

*Carbon-isotopes:*

No data is yet available for C-isotope fractionation in the amine solutions commonly used in $CO_2$ capture. For water, C-isotope fractionation between $CO_2$ gas and bicarbonate is greater at lower temperatures[27]. In terms of carbon capture, this suggests that greater isotopic fractionation will take place during the absorption stage than the desorption stage. Below, we use Rayleigh Fractionation[27] to calculate expected $\delta^{13}C$ values for absorbed and desorbed $CO_2$.

In water at typical amine absorption temperatures (40-60 °C), the bicarbonate-$CO_2$ enrichment factor will be between +4 to +7 ‰[27,68]. If 85-99% of the $CO_2$ dissolves to form bicarbonate in the amine solution, the resulting bicarbonate will be enriched in $^{13}C$ by 0 to +2.34 ‰ relative to the original $CO_2$ flue gas. At desorption temperatures (100-140 °C), the $HCO_3^-$ - $CO_2$ enrichment factor will be ± 1 ‰[68], and if 99% of the bicarbonate is desorbed, the resulting $CO_2$ will have a $\delta^{13}C$ value between -0.06 and +0.06 ‰ compared to that of the saturated bicarbonate. The net enrichment of captured $CO_2$ relative to original flue $CO_2$ will therefore be between -0.06 and +2.4 ‰, depending on the absorption and desorption temperatures.

An isotope fractionation factor of +1.011 (equivalent to an enrichment factor of ~+11 ‰) has been determined for carbamate relative to aqueous $CO_2$[69]. $^{13}C$ enrichment between gaseous and aqueous $CO_2$ in fresh water at typical amine absorption temperatures (40-60 °C) is -0.9 to -1.0 ‰[27] and so the net isotope enrichment factor of carbamate relative to the original $CO_2$ flue gas will be ~ +10 ‰. If 85-99% of the $CO_2$ dissolves to form carbamate in the amine solution, the resulting carbamate will be enriched in $^{13}C$ by +0.5 to +3 ‰ relative to the original flue gas $CO_2$. If 99% of the carbamate is desorbed, the resulting $CO_2$ will be have $\delta^{13}C$ ~ 0.5 ‰ lower than the saturated carbamate, resulting in a net enrichment of $^{13}C$ in the captured $CO_2$ of 0 to +2.5 ‰ relative to the original flue gas.

The anticipated $^{13}C$ enrichment in $CO_2$ from amine capture, relative to the original flue gas $CO_2$, will be between -0.06 and +2.5 ‰, with the exact enrichment value dependant on absorption and desorption

407 temperature, and the relative proportions of bicarbonate and carbamate species in the amine
408 solution.
409
410 However, work investigating C-isotope fractionation during absorption of $CO_2$ by $NH_3$-$NH_4Cl$ solutions
411 at room temperature suggests that, in alkaline solutions, dissolved carbon (bicarbonate and
412 carbamate ions) may be depleted in $^{13}C$ relative to the $CO_2$ gas by more than -50 ‰[70]. In the context
413 of the above discussion regarding absorption / desorption efficiency, this may result in significant $^{13}C$
414 depletion in the captured $CO_2$ relative to the source gas, the opposite effect of what would be
415 expected from dissolution in water.
416
417 The $CO_2$ injected at the Pembina CCS project was derived from the Ferus natural gas processing plant[71],
418 which presumably used a form of chemical absorption to strip $CO_2$ from natural gas. It had $\delta^{13}C$ ~-
419 4.7‰[11], which falls well within the range of values for $CO_2$ co-existing with natural gas (-13.9 to +13.5[72],
420 Fig. 1). Similarly, $CO_2$ captured using amine solvents from steam reforming of methane (see
421 gasification, above) has $\delta^{13}C$ of -37 ‰[49,51], well within the isotopic range of natural gas (-20 to -52 ‰).
422 Given the breadth of possible $\delta^{13}C$ values for the source $CO_2$, these data do not help to constrain which
423 of the above hypotheses is true, but suggest that $^{13}C$ enrichment of the captured $CO_2$ relative to the
424 original $CO_2$ is less than ± 20 ‰. More work to experimentally determine C-isotope fractionation
425 during $CO_2$ capture would be beneficial. In the meantime, we tentatively conclude that fractionation
426 of C-isotopes during amine capture is likely between -20 ‰ and +2.5 ‰ relative to the source $CO_2$,
427 based on the available data for captured $CO_2$ relative to feedstocks, and the likely maximum
428 enrichment calculated for $CO_2$ dissolution in fresh water.
429
430 *Noble gases:*
431 Little data is available for the noble gas content of the $CO_2$ stream produced by chemical absorption.
432 In a summary of the $CO_2$ product stream specifications from a number of post-combustion capture

technologies[73], Ar was present at concentrations of 10-25 ppmv, much lower than the atmospheric concentration of 9340 ppmv (Table 1). This is likely due to the unreactive noble gases remaining in the gas phase during absorption and subsequently being vented, rather than being absorbed with the $CO_2$. A small proportion of the noble gases will dissolve into the amine solution. As noble gas solubility decreases with increasing temperature, these will be efficiently exsolved when the solvent is heated to release the $CO_2$. Noble gas solubility is controlled by Henry's Law with the heavy noble gases having greater solubilities than lighter noble gases. As a result we might expect noble gas element ratios to show heavy element enrichment relative to atmosphere.

**3.7.2 Physical absorption**

Physical absorption of $CO_2$ requires a high partial pressure of $CO_2$ and is often used to separate $CO_2$ from other gases in $CO_2$–rich gas streams, such as the products of gasification processes. $CO_2$ absorption or dissolution into the solvent is according to Henry's Law[74]. No chemical reaction takes place and the absorbed gas is released from the solvent by pressure reduction. Physical absorption using cold methanol is used to capture $CO_2$ produced at the Great Plains Synfuel plant, North Dakota, USA, for use in the Weyburn enhanced oil recovery (EOR) and CCS site[7].

*Carbon isotopes:*

To the best of our knowledge there is no data available to assess the effect of physical absorption on $\delta^{13}C\text{-}CO_2$. However, we would expect an enrichment of $^{13}C$ in the dense phase[27] (i.e. dissolved in the solvent) and the isotopic composition of the resulting captured $CO_2$ will depend on the relative efficiencies of the absorption and desorption mechanisms. If desorption is more efficient than absorption, then a small degree of $^{13}C$ enrichment is likely.

*Noble gases*:

458 In general, noble gases have a much higher solubility in organic solutions than in water[75,76] and follow
459 Henry's Law, with the heavier noble gases having higher solubility. However, as is the case with noble
460 gas dissolution in amine solvents, the noble gases will be preferentially retained in the gas phase and
461 become decoupled from the $CO_2$. The small proportion of noble gases that are absorbed into the
462 solvent will likely be enriched in the heavier noble gases relative to atmosphere due to the enhanced
463 solubility of the heavier noble gases. Assuming efficient desorbing of gases from the physical solvent,
464 $CO_2$ captured via physical absorption is likely to contain low concentrations of noble gases with
465 element ratios enriched in heavy noble gases relative to the noble gas composition of the original flue
466 gas. Isotopic ratios, however, are unlikely to change.
467
468 ***4. Geochemistry of fluids and gases in actual and potential CCS storage sites***
469 The two types of storage sites currently considered to have the most potential for CCS in the short
470 term are depleted oil and gas fields, and deep, saline formations. In geological terms, these two types
471 of storage are very similar, comprising reservoir rocks filled with saline fluid. In the case of depleted
472 hydrocarbon fields, a wealth of information is available from hydrocarbon exploration and the fields
473 are proven to have stored buoyant fluids or gas over geological timescales. On the other hand, many
474 wells may have been drilled in such fields, resulting in potential leakage pathways and many
475 hydrocarbon fields are too small to provide large-scale $CO_2$ storage. Conversely, saline aquifers are
476 much larger, but are poorly studied due to lack of hydrocarbon accumulation and it is not conclusively
477 known whether a given aquifer is leak-tight with respect to buoyant fluids. Porous basalt formations
478 pose another promising storage option[77] but the chemical and transport processes involved in these
479 cases have significant differences compared to storage in sedimentary formations, and are beyond
480 the scope of this review.
481
482 To trace $CO_2$ injected into a storage reservoir, the baseline conditions of the reservoir, and the likely
483 in-reservoir processes need to be known. Hydrodynamically closed reservoirs will tend to have more

stable baseline conditions and predictable behaviour, while hydrodynamically open reservoirs, and depleted hydrocarbon reservoirs that, at best will be contaminated with drilling fluids and at worst may have been flushed with water to aid hydrocarbon recovery, may have spatially and temporally variable baselines and thus exhibit less predictable behaviour. Below we summarise the measured and expected geochemical baselines for potential storage reservoirs. While a reasonable amount of data is available for hydrocarbon reservoirs, less information is available for the baseline evolution after production ceases. Data for non-hydrocarbon bearing saline aquifers are uncommon.

***4.1 Carbon-isotopes:***

The $\delta^{13}C$ of $CO_2$ in storage formations generally varies between ~-23 and +1 ‰ (Figure 2, Supplementary Table S3). Formations that experience rapid flow of formation water, or mixing of water reservoirs may exhibit a large range in $\delta^{13}C_{CO_2}$ values at a single site (e.g. -23 to -16 ‰ at Weyburn[78]). $\delta^{13}C$ for DIC are more constrained, based on the available data, and fall between -9 and +3 ‰ (see supplementary Table S3), regardless of whether the host rock is carbonate or siliciclastic, or whether the storage formation has experienced previous hydrocarbon exploitation, but this may reflect a limited dataset. For storage reservoirs in depleted hydrocarbon fields or associated with EOR, the baseline isotope values may fluctuate strongly depending on industrial activities, such as water flushing[79] or contamination with organic matter resulting in enhanced bacterial action[80].

***4.2 Noble gases:***

The most comprehensive noble gas measurements from a CCS reservoir are from the Weyburn EOR project[81], although these do not represent baseline data. $^4He$ concentrations were 2 orders of magnitude greater than for air saturated water (ASW) while other noble gas isotopes (Ne – Kr) had concentrations 1-2 orders of magnitude lower. The isotopic composition of the noble gases is consistent with a depletion in atmospheric noble gases, as would be expected for a hydrocarbon-rich formation where the noble gases partition into the hydrocarbon phase, rather than the pore-water

phase, and an enrichment in radiogenic isotopes, consistent with a deep-origin of the fluid. Similarly at the Cranfield $CO_2$-EOR site, noble gas data from produced gases indicate high levels of terrigenic / radiogenic $^4$He in the reservoir[82]. Other noble gas data are available for fluids from the Rousse and Frio storage reservoirs. The Frio data are restricted to He and Ar concentrations (80,000 ppb (>> air) and 400,000 ppb (≈ ASW) respectively[48]). Air-normalised concentrations for $^4$He, $^{20}$Ne, $^{36}$Ar, $^{40}$Ar and $^{84}$Kr, from Rousse show that, while the concentration of $^4$He was ~ ten times greater than air, the remaining noble gases were all 100 to 1000 times lower than air, with a positive correlation between concentration and elemental mass[37].

These observations are consistent with the formation waters having interacted with hydrocarbons, causing depletion in atmospheric noble gases (originally derived via hydrologic recharge) relative to expected air saturated water (ASW), due to preferential partitioning into the hydrocarbon phase (Section 2.2). Repeated dissolution and exsolution of noble gases will produce greater degrees of elemental fractionation, with an enrichment of heavy relative to light noble gases, compared to air[83]. While these processes facilitate precise quantitative modelling when all of the relevant conditions are well characterised, it is difficult to place more quantitative constraints on the range of noble gas concentrations that could be expected in deep aquifers.

The isotopic composition of subsurface noble gas elements, however, does not fractionate during dissolution and exsolution and is instead controlled by mixing between different sources of noble gases. In very simplistic terms, the formations likely to be of most interest for CCS are those that have at least some degree of hydrodynamic isolation. In such cases, the fluids in the reservoir will be relatively old, residing in the subsurface for a considerable amount of time, perhaps approaching geological timescales. This will give a much stronger radiogenic and terrigenic noble gas signature than would be observed for shallow, freshwater aquifers that undergo regular recharge (see Section 7). Noble gases in hydrocarbon systems often have a resolvable mantle component identified by elevated

$^{3}$He, and a high proportion of radiogenic isotopes that are often correlated with reservoir depth ($^{4}$He*, $^{21}$Ne*, $^{40}$Ar*, with "*" denoting a radiogenic origin)[30,84–86]. Some hydrocarbon fields have elevated, isotopically atmospheric, Kr and Xe that cannot be explained by elemental fractionation in a water-oil-gas system. This is attributed to adsorption of atmospheric Kr and Xe onto the carbon-rich sediments that are the source of hydrocarbons[30,87]. Such sediment-derived Kr and Xe enrichments may occur in hydrocarbon fields, but would partition into the hydrocarbon phases, rather than water and so are unlikely to be observed in saline aquifers or depleted hydrocarbon fields where the Kr and Xe enriched phase was either never present or has been removed.

In the case of depleted oil and gas fields an additional source of noble gases may be introduced during water-stimulation to maintain reservoir pressure. The extent of this contamination will depend on the relative volumes of water added, amount of original formation water remaining, and the noble gas composition of the injected water. If sea water is injected, as is likely in offshore hydrocarbon fields, the added noble gases will be those of atmosphere equilibrated sea water (similar order of magnitude concentrations to those quoted for fresh water in Table 1). If produced fluids from the field are simply reinjected, then the noble gas composition is unlikely to change.

Many factors control the noble gas composition of potential storage reservoirs and so good noble gas baseline data will be beneficial if noble gases are to be used as tracers. Many reservoirs are likely to have elevated He concentrations relative to air or ASW and be depleted in other noble gases, while isotopic ratios will show strong radiogenic and terrigenic components. Saline aquifers will likely have more stable and consistent baselines than depleted hydrocarbon fields where contamination from production processes is likely.

## 5 Geochemical evolution of the $CO_2$ stream on injection and migration in the subsurface

Once injected into a geological storage formation, the fingerprint of the $CO_2$ stream will change depending on the processes and reactions that take place and the timescale and rate of those reactions. This section describes the changes that are likely to take place as the $CO_2$ plume migrates through the subsurface. Dominant processes will be mixing of the injected $CO_2$ with pre-existing materials, dissolution of the injected $CO_2$ into formation waters, fluid-rock reactions such as dissolution of carbonate minerals, and migration. Precipitation of secondary carbonate and clay minerals will also change the stable isotope composition of the carbon-bearing gases and fluids in the subsurface, but there is currently limited evidence that these processes will occur on site-monitoring timescales and, given the current uncertainties regarding mineral precipitation during $CO_2$ storage, these will not be considered here. Transport of $CO_2$ through the subsurface can be considered in terms of diffusive and advective transport, both of which may affect the composition of the $CO_2$ plume in different ways.

**5.1 Carbon isotopes**

$\delta^{13}C$ evolution of injected $CO_2$ has been covered by a number of recent review papers[11,12,19,23–26] and so is only qualitatively described here. Injected $CO_2$ will first mix with any free-phase $CO_2$ in the reservoir, resulting in a $CO_2$ plume with a $\delta^{13}C$ value resulting from mixing between injected and baseline values. Identification of the injected $CO_2$ plume is thus dependent on the difference between the injected and baseline $\delta^{13}C_{CO_2}$, the relative volumes of injected and baseline $CO_2$, and relevant enrichment factors (which in turn are dependent on temperature and salinity) between gases and dissolved C-species

$CO_2$ will begin to dissolve into the formation water to form dissolved inorganic carbon (DIC), with isotopic fractionation between $CO_2$ and DIC related to temperature, pH and the DIC species formed. At reservoir conditions, DIC derived from the injected $CO_2$ is calculated to be enriched in $^{13}C$ by -1 to +7 ‰ relative to the co-existing $CO_2$[27]. This DIC will subsequently mix with baseline DIC.

587

588 Carbonic acid formation may cause dissolution of any carbonate minerals present, adding another
589 source of C to the DIC; the stable isotope composition of these carbonate minerals, and thus resulting
590 $\delta^{13}C_{DIC}$ depends on the origin of the carbonate (Figure 1).

591

592 Diffusive transport through rock or soil pore networks may cause C-isotope fractionation at the
593 migration front, resulting in sequential $^{13}C$ depletion and then enrichment at a given location as the
594 migration front passes[12,88]. For dry systems, if reactive mineral surfaces such as illite are present,
595 $^{44}[CO_2]$ ($^{12}C^{16}O_2$) may be preferentially adsorbed onto the surfaces, resulting in an initial $^{13}C$ enrichment
596 of the free-phase $CO_2$, that can change the $\delta^{13}C_{CO_2}$ by up to hundreds of permil, followed by $^{12}C$
597 enrichment relative to the bulk $CO_2$ as the $^{12}CO_2$ is desorbed, resulting in lower $\delta^{13}C$ values, before
598 returning to the bulk composition[89]. Further work is needed to investigate the presence of this effect
599 in fluid saturated systems. While these processes are unlikely to affect the bulk of $CO_2$ injected for
600 storage, they may affect the migration front of the injection plume and any $CO_2$ that leaks from the
601 storage site. Early measurements of $\delta^{13}C_{DIC}$ at the Ketzin observation well Ktzi 200 gave $\delta^{13}C$ values
602 lower than expected for mixing of $CO_2$ sources and calculated C- isotope fractionation during
603 dissolution; diffusive fractionation was a speculated cause of this depletion[80].

604

605 **5.2 Noble gases**

606 The processes affecting noble gases in the subsurface are described in a number of recent summary
607 papers and text books[28–30,90,91]. As with stable isotopes, the noble gas signature of the injected $CO_2$
608 stream will first be modified by mixing with any atmospheric, terrigenic and radiogenic noble gas
609 components in the reservoir gas phase. Exchange of noble gases between different reservoir phases
610 (gas, water, oil, solid particles) may take place according to the differences in solubility described in
611 Section 2.2. Note from Table 1 that Xe will partition preferentially into oil rather than gas at
612 temperatures less than 50 °C and so interaction of the injected $CO_2$ with any oil in the subsurface will

613 cause Xe depletion in the gas phase. Recent work[92] experimentally determined noble gas partitioning
614 between supercritical $CO_2$ and water and found deviations relative to ideal gas – water partitioning
615 behaviour that became greater with increasing $CO_2$ density. Ar, Kr and Xe all show an increasing
616 affinity for the $CO_2$ phase with increasing $CO_2$ density, due to enhanced molecular interactions of
617 denser-phase $CO_2$ with the larger, more polarisable noble gases, while He shows decreasing affinity[92].
618
619 Physical adsorption of noble gases onto solid particles, while difficult to quantify due to a lack of
620 experimental data on adsorption properties, may significantly fractionate heavy from light noble gas
621 elements and a number of studies indicate enrichment of Kr and Xe in organic rich shales and
622 coal[29,93,94]
623
624 Migration of the plume-front may chromatographically fractionate the noble gas elements and $CO_2$
625 due to differences in molecular diffusion rate and solubility, although the specific manifestation of this
626 fractionation depends on the rock matrix, the gas transportation mechanism and relative solubility of
627 the gas species. Less soluble species will migrate faster than more soluble species[95], meaning that
628 noble gases, which will preferentially partition into the gas phase, should travel faster through the
629 subsurface than $CO_2$, which will begin to dissolve on contact with water. If gas transport takes place
630 via molecular diffusion through pore space, the lighter, faster diffusing species will travel more quickly
631 through the subsurface than the heavier, slower diffusing species. In the case of arrival of the
632 migration front at a monitoring well, we would expect to detect gases in the following order, with the
633 delay between gas arrival dependant on the distance travelled: He, Ne, Ar, $CO_2$, Kr, Xe[96]. However, the
634 opposite may be true when gas transport is via advection along fractures, with faster-diffusing species,
635 which are more able to enter the rock pore-space, travelling less rapidly than slower diffusing species,
636 which are confined to fractures and more open, faster flow pathways[97]. The isotopic composition of
637 the noble gases, however, is not expected to be altered by migration, and so characterisation of

baseline and injected noble gas isotope compositions will allow mass-balance modelling and fingerprinting of any subsurface samples produced from monitoring wells.

## 6. Past and present use and future potential of inherent tracers for in-reservoir processes in CCS projects

A number of projects have successfully used inherent stable isotopes to monitor $CO_2$ behaviour in the subsurface, while added noble gases have also proven useful. Supplementary Table S4 summarises the ways that these tracers have been used in different CCS projects and identifies the key papers describing these applications. Many of these projects and applications have been summarised in recent review papers[12,17,26].

Using C-isotopes as a $CO_2$ or DIC fingerprint to detect breakthrough and monitor migration of the injected $CO_2$ is the most common application of inherent tracers in existing CCS projects. In most of these projects the injected $CO_2$ was isotopically distinct from baseline $CO_2$ and DIC. However C-isotopes were still a useful tool for monitoring migration and breakthrough at Weyburn, where the injected and baseline $\delta^{13}C_{CO_2}$ overlap (due to the wide range of baseline values), and at Pembina, where the injected $\delta^{13}C_{CO_2}$ overlapped with baseline $\delta^{13}C_{DIC}$ (Figure 2). In these cases, C-isotope fractionation during dissolution of injected $CO_2$ to form bicarbonate (~ 5 ‰ at 50-60 °C) increases the separation in $\delta^{13}C$ values between baseline DIC and injection-derived derived $HCO_3^-$. In many cases (see Supplementary Data Table S4), C-isotopes were the most sensitive tracer, indicating arrival of injected $CO_2$ at a monitoring well earlier than significant changes in fluid pH or $CO_2$ concentration. When the baseline conditions are well characterised, C-isotopes have proven to be useful for quantifying the proportion of $CO_2$ or DIC derived from the injected $CO_2$ and from in-reservoir mineral dissolution (Weyburn[12,98–100], Cranfield[101] and Ketzin[80]). C-isotopes have also proven useful at identifying contamination from drilling fluids[80].

664 Hence, $\delta^{13}C$ of $CO_2$ and DIC has the potential to be a powerful in-reservoir tracer, as long as the injected
665 $CO_2$ has a $\delta^{13}C$ value that is easily distinguishable from background $CO_2$ and, if it dissolves, will produce
666 DIC with $\delta^{13}C$ distinguishable from baseline DIC. Figure 3 compares the expected $\delta^{13}C$ of captured $CO_2$
667 from a number of processes and feedstocks, to the range of likely baseline storage formation values.
668 From this, we can see that C3 biomass and fossil fuel derived $CO_2$ will be easiest to distinguish from
669 reservoir baseline conditions, using $\delta^{13}C$, although coal and C3 biomass derived $CO_2$ have a greater
670 chance of overlap.
671
672 While no studies have taken place using noble gases inherent to captured $CO_2$ as a tracer, use of noble
673 gases co-existing with natural $CO_2$ injected for EOR operations[31] and as added tracers for both tracing
674 $CO_2$ migration (Frio, Ketzin) and quantifying residual saturation (Otway) suggest that noble gases could
675 prove very useful, if their injected composition is different to those of the reservoir baseline. In
676 addition to experimental CCS sites, natural tracers have been used to study reservoir processes in
677 natural $CO_2$ accumulations with combined noble gas and C-isotope measurements identifying $CO_2$
678 dissolution into the formation waters[102].
679
680 **7. Geochemistry of potential leakage reservoirs (atmosphere, soil and groundwater aquifers)**
681 The aim of CCS is to prevent $CO_2$ from entering the atmosphere and so being able to detect seepage
682 of geologically stored $CO_2$ to the atmosphere is a high priority. However, this remains difficult due to
683 problems associated with identification of leakage sites, leakage plume dilution, and difficulties in
684 establishing a precise local atmospheric baseline. In this section we will briefly review the probable
685 range of baseline conditions for C-isotopes and noble gases in the reservoirs most likely to be
686 influenced by $CO_2$ leakage and how these may or may not contrast with $CO_2$ leakage signatures.
687
688 **7.1 Atmosphere**
689 *C-isotopes*

690 Atmospheric $CO_2$ has $\delta^{13}C$ of between -6 and -8 ‰ V-PDB[27] (Figure 1), but may vary spatially and
691 temporally with local conditions, weather, and anthropogenic activity; e.g. atmospheric
692 measurements in Dallas, Texas, ranged from $\delta^{13}C_{CO_2}$ of -12 to -8 ‰ over ~ 1.5 years due to varying
693 photosynthetic uptake, respiration and anthropogenic sources (vehicle emissions)[103]. C-isotopes can
694 be a sensitive tracer, despite large background fluctuations, by using Keeling plots, which correlate
695 $\delta^{13}C_{CO_2}$ with inverse $CO_2$ concentration to determine the isotopic composition of local $CO_2$ (ecosystem
696 respired and anthropogenic sources) mixing with regional atmospheric $CO_2$[104]. If injected $CO_2$ were to
697 leak to the atmosphere from the subsurface, it should be identifiable using Keeling plots as long as its
698 $\delta^{13}C$ is different to that of the (previously established) baseline end members. Keeling plots from North
699 and South America suggest that ecosystem respired $CO_2$ has $\delta^{13}C$ between -33 and -19 ‰[104], which is
700 similar to the anticipated $\delta^{13}C$ of $CO_2$ captured from burning C3 biomass and some fossil fuels; $\delta^{13}C$ of
701 captured $CO_2$ may thus be especially difficult to distinguish from surface $CO_2$. Captured $CO_2$ derived
702 from natural gas combustion may be depleted enough in $^{13}C$ and $CO_2$ captured from natural gas
703 processing plants may be sufficiently enriched in $^{13}C$ to be distinguishable from local and regional
704 atmospheric sources of $\delta^{13}C$.
705
706 *Noble gases:*
707 The concentration of noble gases in the atmosphere is given in Table 1. Atmospheric values for
708 commonly used noble gas isotopic ratios include: $^3He/^4He$ = 1 $R/R_A$[105]; $^{20}Ne/^{22}Ne$ = 9.8[105];
709 $^{40}Ar/^{36}Ar$=298.56[106]. Regardless of the inherent noble gas composition of the injected $CO_2$ stream, if
710 $CO_2$ leaks from deep geological storage it will most likely be accompanied by baseline reservoir noble
711 gases, which will be enriched in radiogenic and terrigenic isotopes (e.g. $^3He/^4He << 1$ $R/R_A$; $^{40}Ar/^{36}Ar >$
712 298.56).
713
714 **7.2 Soil**
715 *C-isotopes*

As with atmosphere, the stable isotope composition of soil $CO_2$ can vary spatially and temporally with local conditions. It is governed by a combination of $CO_2$ produced by soil respiration, fractionation during diffusion, mixing with atmospheric $CO_2$ and by isotopic exchange with soil water[88,107]. This can result in highly variable $\delta^{13}C$ values for soil that vary on a daily basis. $\delta^{13}C$ data are available for soil from a number of CCS sites (Supplementary Table S5), all of which show more than 10 ‰ variation (between -27 and -7 ‰) with no evidence of being contaminated by injected $CO_2$. There is considerable overlap between the $\delta^{13}C$ of soil $CO_2$ and the expected range of $\delta^{13}C$ values of captured $CO_2$ (Figure 3). $CO_2$ derived from combustion or gasification of natural gas may produce $CO_2$ significantly more depleted in $^{13}C$ than soil $CO_2$, while $CO_2$ captured from natural gas processing may be significantly enriched. Given the wide variation in baseline soil $\delta^{13}C$ values at any given site, C-isotopes in isolation will only be a useful leakage tracer if the leaking $CO_2$ has a distinctive $\delta^{13}C$ (i.e. derived from natural gas or natural gas processing), and if $CO_2$ concentration is also measured and Keeling Plots are used. Use of $\delta^{13}C_{CO_2}$ in conjunction with concentrations of oxygen and nitrogen can be a useful tool to identify mixing between atmospheric $CO_2$ and $CO_2$ produced in the soil from biological respiration or methane oxidation[108].

*Noble gases*

In simplistic terms, noble gases in soil are derived from the atmosphere and partition between gas and water phases; soil gas should have an atmospheric noble gas composition, while fluids have concentrations consistent with air saturated water (ASW) for the local soil temperature[109]. However, this ideal theoretical behaviour is not always observed. Changes to the local combined partial pressure of $CO_2$ and $O_2$ (due to the greater solubility of $CO_2$ over $O_2$) can cause corresponding changes to noble gas concentrations and elemental ratios, with heavier noble gases more affected than lighter noble gases, likely due to differences in diffusion rate[90], though isotopic ratios remain atmospheric. Three soil gas monitoring projects associated with CCS sites provide limited noble gas concentration data (Supplementary Table S5). At Weyburn, Ar concentrations[110] are atmospheric (~0.9%) and at Rousse,

He concentrations from four separate campaigns were consistent at ~ 5 ppm[111], again consistent with atmospheric concentrations. At Otway, baseline He concentrations in the soil ranged from 3 to 103 ppm[112,113] i.e. ranging between enriched and slightly depleted compared to atmosphere. The reasons for these elevated He concentrations were unknown, but not thought to represent leakage of a deep gas source.

In terms of using noble gases to detect leaking $CO_2$, isotopic ratios will be the most useful tool. The isotopic ratios of noble gases in baseline soil will be atmospheric (see above), while noble gases in $CO_2$ leaking from depth will most likely have $^3He/^4He$ below atmospheric values, and $^{40}Ar/^{36}Ar$ greater than atmosphere, irrespective of the noble gas composition of the injected $CO_2$, due to enrichment of radiogenic $^4He^*$ and $^{40}Ar^*$ in the subsurface (see Sections 2.2 and 4). Concentrations of noble gas elements or isotopes may provide additional information, depending on the noble gas content of the injected $CO_2$, and as long as variations in baseline soil noble gas partial pressure and elemental fractionation due to changing $CO_2 + O_2$ content are taken into account.

**7.3 Shallow aquifers**

Shallow aquifers are often sources of potable water and hence $CO_2$ leakage into such reservoirs is undesirable. Such reservoirs are recharged by meteoric water, are thus hydrodynamically connected to the surface and so leakage of $CO_2$ into a shallow aquifer will likely result in escape of some of that $CO_2$ to the atmosphere. For these reasons, identification and mitigation of any $CO_2$ leakage into shallow aquifers will be a high priority.

Compared to the atmosphere or soil, baseline geochemical conditions in aquifers are likely to be much more stable, thus providing a higher sensitivity for leak detection. Furthermore, if the hydrodynamic gradient of an aquifer is well characterised, monitoring wells can be placed downstream of any

767 potential leakage structures, allowing efficient monitoring of a relatively large area without the need
768 to identify and monitor every single potential leakage point[114].
769
770 *C-isotopes*
771 The $\delta^{13}C$ value of $CO_2$ and DIC in fresh spring and groundwaters is generally derived during recharge
772 from the soil, followed by dissolution, associated isotope fractionation (see Section 5) and weathering
773 of carbonate material[27]. Bacterial action can isotopically enrich DIC in $^{13}C$ (up to +30 ‰), via reduction
774 of $CO_2$ to methane (Figure 1), or fermentation of acetate to produce $CH_4$ and $CO_2$[115–118].
775
776 Supplementary Table S5 lists $\delta^{13}C$ for $CO_2$ and DIC in selected freshwater springs and aquifers. Data
777 for Ketzin, Altmark, Otway and Hontomín were collected as part of CCS monitoring programmes. $\delta^{13}C$
778 values of both $CO_2$ and DIC range from -24 to -9 ‰, consistent with derivation from soil $CO_2$ (Figure
779 1). Data from other aquifers extend the range to higher values, indicating bacterial action. $\delta^{13}C$ of $CO_2$
780 in shallow aquifers may be difficult to distinguish from $\delta^{13}C_{CO_2}$ of captured and injected $CO_2$, especially
781 that derived from coal and biomass feedstocks and cement manufacture.
782
783 *Noble gases*
784 Noble gases enter subsurface aquifers via recharge of meteoric water in the vadose zone of soils and
785 baseline compositions reflect air saturated water (ASW), with or without excess air, for the local soil
786 temperature[109]. While deviations from this ideal behaviour have been noted, these are most likely
787 explained by changes to noble gas partial pressure in soil, described above[90]. In general, the processes
788 that result in noble gas elemental fractionation in meteoric and groundwater are controlled by well
789 understood physical mechanisms, are related to the residence time of water in the subsurface, and
790 can be modelled[32]. Groundwater may thus provide a well constrained, predictable baseline for leakage
791 monitoring using noble gases. Furthermore, as noble gases are sparingly soluble in water, the
792 concentration of noble gases in ASW is significantly lower than that of the atmosphere, resulting in a

793 signal to noise ratio that is 100 times more sensitive[119]. While the processes controlling the noble gas
794 content of groundwater are well understood and their behaviour predictable, they are dependent on
795 specific local recharge conditions, and so establishing a precise baseline is essential. As with
796 atmospheric and soil reservoirs, the baseline of recently recharged aquifers is likely to differ from
797 leaking $CO_2$ by a lack of radiogenic and terrigenic noble gases. However, old (hundreds of thousands
798 of years) groundwaters may exist in aquifers used as domestic and agricultural water sources, and
799 such aquifers may have significant radiogenic and terrigenic components. One such example is the
800 Milk River aquifer in Alberta, Canada, which has groundwater residence times of up to 500 ka[120]. The
801 majority of noble gases have concentrations between 0.2 and 4 times the expected values for ASW,
802 but radiogenic and terrigenic-derived $^{4}He$ is enriched in some wells by more than 2000 times the
803 expected ASW value and $^{40}Ar/^{36}Ar$ values are all greater than atmosphere[121].
804
805 **8. Past and present use and future potential of inherent tracers for leak detection in CCS projects**
806 Use of tracers for monitoring leakage of $CO_2$ into overlying reservoirs (aquifers, soil, atmosphere)
807 follows the same principles as for in-reservoir monitoring, but with the added complication that the
808 released volumes are likely to be much smaller and so sensitivity and detection become a critical issue.
809 Geochemical analysis is a common monitoring technique for CCS sites, many of which employ surface,
810 soil and / or groundwater analysis to monitor for leakage or contamination and a recent review[19]
811 provides more details on the theory and practice of using tracers to detect $CO_2$ leakage into freshwater
812 aquifers. However, in the vast majority of CCS field tests, no leakage has been observed and these
813 projects are thus of limited value in assessing the viability of using inherent tracers as leakage
814 detection. An exception is the Frio CCS project, where added tracers, elevated dissolved $CO_2$ gas
815 contents, slight increases in $HCO_3^-$ concentrations and substantial depletion in $^{13}C$ of DIC were found
816 in strata above a primary seal (but remaining below the main structural trap for the storage reservoir),
817 indicating that $CO_2$ had leaked within the subsurface[48]. These indicators returned to background levels
818 within nine months of injection, suggesting that the leak was short-lived and occurred early in the

injection process. Given that the injection well was 50 years old, leakage from the well itself was considered to be the most likely source of the $CO_2$, rather than migration between strata[48]. While it was not possible to calculate the volumes of leaked $CO_2$ at Frio, it seems that C-isotopes of DIC may provide a potentially powerful tracer of $CO_2$ leakage when volumes are so low that there is no significant rise in $HCO_3^-$ concentration.

At the Rangely-Weber $CO_2$-EOR site, Colorado, $CO_2$ and $CH_4$ gas fluxes were used to quantify micro-seepage from the reservoir[122]. Statistical analysis showed that gas flux and isotopic composition was different between the area overlying the reservoir, and a nearby control site, but it was not possible to conclusively attribute these differences to gas seepage from the reservoir. Assuming that the differences were due to gas seepage, maximum seepage rates of 170 tonnes per year $CO_2$ and 400 tonnes per year $CH_4$ were calculated[122].

Allegations of $CO_2$ leakage from the Weyburn EOR site into farmland (the Kerr Property) were shown to be unfounded[123], but this case study provides useful insights of how natural tracers can help to determine the origin of $CO_2$, even when robust baseline data is not available. A number of incidents and $CO_2$ measurements led the owners of the farmland to believe that $CO_2$ injected into the Weyburn site was leaking into their property. One of the reasons for this belief highlights a potential downfall of using stable isotope data for tracing $CO_2$ migration; high concentrations of $CO_2$ measured in the soil had the same $\delta^{13}C_{CO_2}$ as the $CO_2$ being injected as part of the Weyburn project. This $\delta^{13}C_{CO_2}$ value (~ -21 ‰) was, however, comparable to typical soil gas $CO_2$ compositions[124] (c.f. Figure 1). An independent investigation was commissioned to determine the origin of $CO_2$ on the site, the results of which showed without doubt that the $CO_2$ was natural and did not derive from injection of $CO_2$ for storage or EOR at Weyburn[124]. For soil gas, correlations of $CO_2$ with $O_2$ and $N_2$ were consistent with a $CO_2$ origin by soil respiration, rather than addition of an extra $CO_2$ component, and correlating $CO_2$ concentration with $\delta^{13}C_{CO_2}$ showed that the soil gas isotope composition was easily explained by

845 mixing between atmospheric $CO_2$ and soil gas $CO_2$ with a $\delta^{13}C_{CO_2}$ of -25 ‰[124]. Noble gas and C-isotope
846 analyses on groundwater well samples, injected $CO_2$ and water and fluids produced from deep in the
847 Weyburn formation confirmed that gas from the reservoir was not present[81]. Noble gas
848 concentrations in the shallow groundwaters were consistent with air-saturated water (ASW), as would
849 be expected for the local groundwater system, while the fluids produced from the Weyburn field were
850 very different; most noble gas concentrations (Ne, Ar, Kr, Xe) in the Weyburn fluids were much lower
851 than would be expected for ASW, while $^4He$ concentrations were much higher, consistent with
852 enrichment of radiogenic $^4He$ in the crust[81]. Furthermore, $^3He/^4He$ ratios in groundwater samples were
853 indistinguishable from air, while Weyburn fluids had $^3He/^4He$ values an order of magnitude lower, due
854 to addition of crustal radiogenic $^4He$[81]. Importantly, Weyburn reservoir water and shallow
855 groundwater samples showed no correlation on a plot of $HCO_3^-$ vs $^3He/^4He$, which would be expected
856 if mixing occurred between deep, Weyburn fluids and ASW groundwater[81].
857
858 In the absence of real $CO_2$ leaks from storage sites, information on tracer behaviour during leakage
859 can only be gleaned from controlled release experiments (i.e. injecting $CO_2$ into a unit that will leak)
860 and studying natural $CO_2$ or natural gas seeps. Experiments releasing $CO_2$ into soil at a rate comparable
861 to 0.001% leakage from a 200 Mt $CO_2$ storage site have been successful at identifying $CO_2$ leakage
862 using $\delta^{13}C$ with Keeling plots in both atmosphere and soil, although in these cases the injected $CO_2$
863 had a particularly light isotopic signature ($\delta^{13}C$ <-45 ‰)[35,125–127]. An experimental $CO_2$ leak ($\delta^{13}C_{CO_2}$ -
864 26.6 ‰) into sediments in the North Sea (QICS project) showed that $\delta^{13}C_{DIC}$ of pore water registered
865 the leak earlier than significant increases in $HCO_3^-$ concentration were detected[128]. In these examples
866 the difference in $\delta^{13}C$ between baseline and injected $CO_2$ was 15 to 25 ‰. In these leakage
867 experiments the migration distance for the injected $CO_2$ is small (maximum 11 m – QICS) and it is
868 possible that the isotopic composition of the $CO_2$ could change during migration over the larger
869 distances associated with geological storage (kilometres deep). However, detailed modelling of
870 potential leakage at the QUEST CCS project, Edmonton, Canada, from the Basal Cambrian Sandstone

(BCS) storage reservoir into overlying aquifers indicated that the $\delta^{13}C_{CO_2}$ of the leaking $CO_2$ would differ from the injected $CO_2$ by less than 1 ‰[51].

Another experiment released $CO_2$ with He and Kr tracers into the vadose zone of limestone and showed that molecular diffusivity was not an adequate model for coupled $CO_2$ - tracer behaviour; while He and Kr behaved according to predictive models, the $CO_2$ took significantly longer to travel through the substrate[96]. This experiment gives weight to the hypothesis that noble gases may provide an early warning of $CO_2$ leakage. Further evidence suggesting that noble gases may be useful tracers of $CO_2$ migration comes from studies on natural $CO_2$ and gas seeps. At St John's, Arizona / New Mexico, USA, $\delta^{13}C$ was inconclusive in establishing the origin of elevated $HCO_3^-$ in spring water, but He and Ne isotopes identified both mantle and crustal components and thus a deep origin for the $CO_2$[129]. He and Ne isotopes were similarly used to confirm that elevated levels of soil-gas $CO_2$ and $CH_4$ were due to micro-seepage of gas from deep, hydrocarbon-bearing formations at Teapot Dome, Wyoming[119]. Importantly, this study established that total He concentrations of approximately just 10 ppm in soil gas and 0.1 ppm in groundwater aquifers would be sufficient to identify deep-sourced He[119].

In summary, C-isotopes may be useful for detection of leakage and seepage if the baseline and injected $CO_2$ are significantly different. When isotopic compositions are not distinctive, combining $\delta^{13}C$ with $CO_2$, $O_2$ and $N_2$ concentrations can help to constrain the $CO_2$ origin. Of the noble gases, He is a particularly sensitive leak and seep tracer due to its low background concentrations at the surface and likely high concentration in the storage reservoir, regardless of the He content of the injected $CO_2$.

**9. Summary, Implications and Conclusions:**

The inherent stable isotope and noble gas composition of captured $CO_2$ has the potential to provide powerful monitoring tools for carbon capture and storage projects, both for in-reservoir processes and for identifying leakage and seepage from the storage unit. This application requires significant

compositional differences between the injected $CO_2$ and the reservoir (for in-reservoir monitoring) and between the reservoir plus injected $CO_2$ and overlying shallow aquifers, soil and atmosphere (for seepage monitoring).

In simplistic terms, captured $CO_2$ is generated in two stages: 1) initial reaction of a feedstock to produce a $CO_2$-bearing flue gas and 2) separation of the $CO_2$ from the other flue gases. When considering the likely isotopic and noble gas composition of the captured $CO_2$ stream, we found that the C-isotope composition and noble gas isotope ratios will be dominated by the initial feedstock, and noble gas concentrations will be controlled by the use of $CO_2$ purification technology.

For fossil fuel and C3 biomass feedstocks a $\delta^{13}C$ fractionation of -1.3 ‰ from the feedstock can be expected while the combustion of C4 biomass may result in greater isotope fractionation. There is a notable lack of information regarding the effect of $CO_2$ separation technologies (e.g. amine capture) on the stable isotope composition of captured $CO_2$ but $^{13}C$ depletion by tens of permil is hypothetically possible. Combining hypothetical considerations with the small amount of available data suggests that C-isotope fractionation during amine capture will be between -20 and +3 ‰. This amounts to a total fractionation between the feedstock and the captured $CO_2$ of between -21 and +2 ‰. A lack of solubility data for noble gases in amine solvents and a lack of detailed noble gas measurements on captured $CO_2$ makes it difficult to predict the noble gas content. Fossil fuel feedstocks are likely to be enriched in radiogenic or terrigenic noble gases (especially $^4He$), and this isotopic component will be transferred to the $CO_2$, although any $CO_2$-purification processes are likely to cause noble gas depletion. However there is a growing body of evidence to suggest that oxyfuel $CO_2$ (and other processes that use cryogenic oxygen, such as Syngas plants) may be enriched in heavy noble gases Kr and Xe. While fossil fuels remain the dominant feedstock, $CO_2$ captured from power plants will likely have a high $^4He$ content (at least before amine capture), but this will change over time if fossil fuels are increasingly replaced with biomass to provide renewable energy with potentially negative $CO_2$ emissions.

923

924 Likely baseline compositions for storage reservoirs and overlying aquifers, soil and atmosphere were
925 reviewed to assess the likelihood that injected $CO_2$ will be isotopically different and this is summarised
926 in Figure 3. Use of fossil fuels and C3 biomass feedstocks are most likely to produce captured $CO_2$ with
927 $\delta^{13}C$ distinctive from baseline conditions, although $\delta^{13}C$ of the $CO_2$ in some storage reservoirs may be
928 difficult to distinguish from coal or C3 biomass derived $CO_2$. $CO_2$ generated from C4 biomass,
929 fermentation, cement manufacture and natural gas processing will be more difficult to distinguish.
930 Elevated $^4He$ concentrations that are expected to occur in various sources of captured $CO_2$ are unlikely
931 to contrast with storage reservoir baseline conditions due to the presence of radiogenic and terrigenic
932 $^4He$, but may provide a highly sensitive tracer for detecting leakage and seepage. Elevated Kr and Xe
933 in $CO_2$ captured from processes that use cryogenic oxygen may be useful, but there is not yet enough
934 data to assess how ubiquitous this enrichment is and whether the concentrations involved are
935 sufficient to allow detection in the reservoir. We note, however, that the wide range of noble gas
936 element and isotope ratios that can be measured means that detailed baseline characterisation of
937 reservoir and injected $CO_2$ is likely to yield some combination of noble gas ratios that provide a suitable
938 in-reservoir tracer.

939

940 A number of fundamental questions remain unanswered due to a lack of empirical data. While we
941 have tried to address these questions hypothetically, more research is necessary to test these
942 hypotheses. Specifically, 1) Will carbon capture technologies result in low noble gas concentrations
943 with preferential loss of light noble gases, and how much C-isotope fractionation will take place during
944 carbon capture? 2) Will $CO_2$ captured from oxyfuel plants have a higher noble gas content than amine-
945 captured $CO_2$, especially for heavy noble gases? 3) Will migration of the $CO_2$ plume over geological
946 distances result in significant fractionation of stable isotopes or noble gases, over what timescales and
947 distance will this fractionation be observed and how might this affect our ability to identify $CO_2$ leakage
948 or seepage?

**Acknowledgements**

This work was supported by EPSRC grant number EP/K036033/1. Editor Daniel Giammar and five anonymous reviewers are thanked for their comments and discussion.

**Supporting Information Available**

Information regarding feedstock composition and gasification processes and supporting information tables are provided in 1 × word document and 1 × excel spreadsheet. This information is available free of charge via the Internet at http://pubs.acs.org.

**References**

(1) Intergovernmental Panel on Climate Change. Climate Change 2013: The Physical Science Basis: Working Group I contribution to the fifth assessment report of the intergovernmental panel on climate change.; Cambridge University Press: Cambridge, UK, 2013.

(2) Intergovernmental Panel on Climate Change. Climate change 2007: Mitigation. Contribution of Working group III to the Fourth Assessment Report of the Intergovernmental Panel on Climate Change.; Metz, B., Davidson, O. R., Bosch, P. R., Dave, R., Meyer, L. A., Eds.; Cambridge University Press: Cambridge, UK, 2007.

(3) Intergovernmental Panel on Climate Change. Climate Change 2001: The Scientific Basis, Summary for Policymakers and Technical Summary of the Working Group I Report; Cambridge University Press: Cambridge, UK, 2001.

(4) Intergovernmental Panel on Climate Change. The Science of Climate Change, Summary for Policymakers and Technical Summary of the Working Group I report; Cambridge University Press: Cambridge, UK, 1996.

(5) International Energy Agency. Energy Technology Perspectives 2014; Executive Summary; Paris, 2014; p 14 pp.

(6) Azar, C.; Johansson, D. J. A.; Mattsson, N. Meeting global temperature targets—the role of bioenergy with carbon capture and storage. Environmental Research Letters **2013**, 8 (3), 34004.

(7) Metz, B.; Davidson, O.; de Coninck, H.; Loos, M.; Meyer, L. IPCC Special Report on Carbon Capture and Storage; Cambridge University Press, 2005.

(8) Pipitone, G.; Bolland, O. Power generation with $CO_2$ capture: Technology for CO2 purification. International Journal of Greenhouse Gas Control **2009**, 3 (5), 528–534.

(9) Aspelund, A.; Jordal, K. Gas conditioning—The interface between CO2 capture and transport. International Journal of Greenhouse Gas Control **2007**, 1 (3), 343–354.

(10) European Parliament. DIRECTIVE 2009/31/EC OF THE EUROPEAN PARLIAMENT AND OF THE COUNCIL of 23 April 2009 on the geological storage of carbon dioxide and amending Council Directive 85/337/EEC, European Parliament and Council Directives 2000/60/EC, 2001/80/EC, 2004/35/EC, 2006/12/EC, 2008/1/EC and Regulation (EC) No 1013/2006. 2009.

(11) Johnson, G.; Mayer, B.; Nightingale, M.; Shevalier, M.; Hutcheon, I. Using oxygen isotope ratios to quantitatively assess trapping mechanisms during $CO_2$ injection into geological reservoirs: The Pembina case study. Chemical Geology **2011**, 283 (3–4), 185–193.

(12) Mayer, B.; Humez, P.; Becker, V.; Dalkhaa, C.; Rock, L.; Myrttinen, A.; Barth, J. A. C. Assessing the usefulness of the isotopic composition of $CO_2$ for leakage monitoring at CO2 storage sites: A review. International Journal of Greenhouse Gas Control **2015**, 37, 46–60.
(13) White, D. J.; Hirsche, K.; Davis, T.; Hutcheon, I.; Adair, R.; Burrowes, S.; Graham, S.; Bencini, R.; Majer, E.; Maxwell, S. C. Theme 2: Prediction, monitoring and verification of $CO_2$ movements. In IEA HGH Weyburn $CO_2$ Monitoring and Storage Project Summary Report 2000-2004; Wilson, M., Monea, M., Eds.; Petroleum Technology Research Centre, 2004; Vol. III, pp 15–69.
(14) Bielicki, J. M.; Peters, C. A.; Fitts, J. P.; Wilson, E. J. An examination of geologic carbon sequestration policies in the context of leakage potential. International Journal of Greenhouse Gas Control **2015**, 37, 61–75.
(15) National Energy Technology Laboratory. Monitoring, Verification, and Accounting of $CO_2$ Stored in Deep Geologic Formations.; DOE/NETL-311/081508; 2009; p 132 pp.
(16) Wells, A. W.; Diehl, J. R.; Bromhal, G.; Strazisar, B. R.; Wilson, T. H.; White, C. M. The use of tracers to assess leakage from the sequestration of CO2 in a depleted oil reservoir, New Mexico, USA. Applied Geochemistry **2007**, 22 (5), 996–1016.
(17) Myers, M.; Stalker, L.; Pejcic, B.; Ross, A. Tracers – Past, present and future applications in $CO_2$ geosequestration. Applied Geochemistry **2013**, 30, 125–135.
(18) Nimz, G. J.; Hudson, G. B. The use of noble gas isotopes for monitoring leakage of geologically stored $CO_2$. In carbon dioxide capture for storage in deep geologic formations - results from the $CO_2$ capture project, vols 1 and 2: vol 1 - capture and separation of carbon dioxide from combustion, vol 2 - geologic storage of carbon dioxide with monitoring and verification; Thomas, D. C., Benson, S. M., Eds.; 2005; pp 1113–1128.
(19) Humez, P.; Lions, J.; Négrel, P.; Lagneau, V. $CO_2$ intrusion in freshwater aquifers: Review of geochemical tracers and monitoring tools, classical uses and innovative approaches. Applied Geochemistry **2014**, 46, 95–108.
(20) Ljosland, E.; Bjørnstad, T.; Dugstad, Ø.; Hundere, I. Perfluorocarbon tracer studies at the Gullfaks field in the North Sea. Journal of Petroleum Science and Engineering **1993**, 10 (1), 27–38.
(21) Stalker, L.; Myers, M. Tracers – Pilot versus Commercial Scale Deployment for Carbon Storage. Energy Procedia **2014**, 63, 4199–4208.
(22) Watson, T. B.; Sullivan, T. Feasibility of a Perfluorocarbon tracer based network to support Monitoring, Verification, and Accounting of Sequestered $CO_2$. Environmental Science & Technology **2012**, 46 (3), 1692–1699.
(23) Becker, V.; Myrttinen, A.; Blum, P.; van Geldern, R.; Barth, J. A. C. Predicting $\delta^{13}C_{DIC}$ dynamics in CCS: A scheme based on a review of inorganic carbon chemistry under elevated pressures and temperatures. International Journal of Greenhouse Gas Control **2011**, 5 (5), 1250–1258.
(24) Kharaka, Y. K.; Cole, D. R.; Thordsen, J. J.; Gans, K. D.; Thomas, R. B. Geochemical Monitoring for Potential Environmental Impacts of Geologic Sequestration of $CO_2$. Reviews in Mineralogy and Geochemistry **2013**, 77 (1), 399–430.
(25) Myrttinen, A.; Becker, V.; Barth, J. A. C. A review of methods used for equilibrium isotope fractionation investigations between dissolved inorganic carbon and $CO_2$. Earth-Science Reviews **2012**, 115 (3), 192–199.
(26) Nowak, M.; Myrttinen, A.; van Geldern, R.; Becker, V.; Mayer, B.; Barth, J. A. C. A brief overview of isotope measuremenets carried out at various CCS pilot sites worldwide. In Clean Energy Systems in the Subsurface: Production, Storage and Conversion; Hou, M. Z., Xie, H., Were, P., Eds.; Springer Series in Geomechanics and Geoengineering; Springer Berlin Heidelberg: Berlin, Heidelberg, 2013; pp 75–87.
(27) Clark, I. D.; Fritz, P. Environmental Isotopes in hydrogeology; 1997.

(28) Aeschbach-Hertig, W.; Solomon, D. K. Noble Gas Thermometry in Groundwater Hydrology. In The Noble Gases as Geochemical Tracers; Burnard, P., Ed.; Springer Berlin Heidelberg: Berlin, Heidelberg, 2013; pp 81–122.
(29) Prinzhofer, A. Noble Gases in Oil and Gas Accumulations. In The Noble Gases as Geochemical Tracers; Burnard, P., Ed.; Springer Berlin Heidelberg: Berlin, Heidelberg, 2013; pp 225–247.
(30) Ballentine, C. J.; Burgess, R.; Marty, B. Tracing Fluid Origin, Transport and Interaction in the Crust. Reviews in Mineralogy and Geochemistry **2002**, 47 (1), 539–614.
(31) Kipfer, R.; Aeschbach-Hertig, W.; Peeters, F.; Stute, M. Noble Gases in Lakes and Ground Waters. Reviews in Mineralogy and Geochemistry **2002**, 47 (1), 615–700.
(32) Widory, D. Combustibles, fuels and their combustion products: A view through carbon isotopes. Combustion Theory and Modelling **2006**, 10 (5), 831–841.
(33) Warwick, P. D.; Ruppert, L. F. Carbon and oxygen isotopes of coal and carbon dioxide derived from laboratory coal combustion. International Journal of Coal Geology **2016**.
(34) Moni, C.; Rasse, D. P. Detection of simulated leaks from geologically stored $CO_2$ with $^{13}C$ monitoring. International Journal of Greenhouse Gas Control **2014**, 26, 61–68.
(35) Turekian, V. C.; Macko, S.; Ballentine, D.; Swap, R. J.; Garstang, M. Causes of bulk carbon and nitrogen isotopic fractionations in the products of vegetation burns: laboratory studies. Chemical Geology **1998**, 152 (1–2), 181–192.
(36) Garcia, B.; Billiot, J. H.; Rouchon, V.; Mouronval, G.; Lescanne, M.; Lachet, V.; Aimard, N. A Geochemical Approach for Monitoring a $CO_2$ Pilot Site: Rousse, France. A Major gases, $CO_2$ - Carbon Isotopes and Noble Gases Combined Approach. Oil & Gas Science and Technology – Revue d'IFP Energies nouvelles **2012**, 67 (2), 341–353.
(37) Bhagavatula, A.; Huffman, G.; Shah, N.; Romanek, C.; Honaker, R. Source apportionment of carbon during gasification of coal–biomass blends using stable carbon isotope analysis. Fuel Processing Technology **2014**, 128, 83–93.
(38) Bottinga, Y. Calculated fractionation factors for carbon and hydrogen isotope exchange in the system calcite-carbon dioxide-graphite-methane-hydrogen-water vapor. Geochimica et Cosmochimica Acta **1969**, 33 (1), 49–64.
(39) Brasseur, A.; Antenucci, D.; Bouquegneau, J.-M.; Coëme, A.; Dauby, P.; Létolle, R.; Mostade, M.; Pirlot, P.; Pirard, J.-P. Carbon stable isotope analysis as a tool for tracing temperature during the El Tremedal underground coal gasification at great depth. Fuel **2002**, 81 (1), 109–117.
(40) Richet, P.; Bottinga, Y.; Javoy, M. A Review of Hydrogen, Carbon, Nitrogen, Oxygen, Sulphur, and Chlorine Stable Isotope Fractionation Among Gaseous Molecules. Annual Review of Earth and Planetary Sciences **1977**, 5 (1), 65–110.
(41) Dufaux, A.; Gaveau, B.; Letolle, R.; Mostade, M.; Noel, M.; Pirard, J. Modelling of the underground coal gasification process at Thulin on the basis of thermodynamic equilibria and isotopic measurements. Fuel **1990**, 69 (5), 624–632.
(42) Du, J.; Jin, Z.; Xie, H.; Bai, L.; Liu, W. Stable carbon isotope compositions of gaseous hydrocarbons produced from high pressure and high temperature pyrolysis of lignite. Organic Geochemistry **2003**, 34 (1), 97–104.
(43) Shuai, Y.; Zhang, S.; Peng, P.; Zou, Y.; Yuan, X.; Liu, J. Occurrence of heavy carbon dioxide of organic origin: Evidence from confined dry pyrolysis of coal. Chemical Geology **2013**, 358, 54–60.
(44) Martens, S.; Kempka, T.; Liebscher, A.; Lüth, S.; Möller, F.; Myrttinen, A.; Norden, B.; Schmidt-Hattenberger, C.; Zimmer, M.; Kühn, M. Europe's longest-operating on-shore CO2 storage site at Ketzin, Germany: a progress report after three years of injection. Environmental Earth Sciences **2012**, 67 (2), 323–334.

(45) Nowak, M. E.; van Geldern, R.; Myrttinen, A.; Zimmer, M.; Barth, J. A. C. High-resolution stable carbon isotope monitoring indicates variable flow dynamic patterns in a deep saline aquifer at the Ketzin pilot site (Germany). Applied Geochemistry **2014**, 47, 44–51.
(46) Hovorka, S. D.; Benson, S. M.; Doughty, C.; Freifeld, B. M.; Sakurai, S.; Daley, T. M.; Kharaka, Y. K.; Holtz, M. H.; Trautz, R. C.; Nance, H. S.; et al. Measuring permanence of CO2 storage in saline formations: the Frio experiment. Environmental Geosciences **2006**, 13 (2), 105–121.
(47) Kharaka, Y. K.; Thordsen, J. J.; Hovorka, S. D.; Seay Nance, H.; Cole, D. R.; Phelps, T. J.; Knauss, K. G. Potential environmental issues of CO2 storage in deep saline aquifers: Geochemical results from the Frio-I Brine Pilot test, Texas, USA. Applied Geochemistry **2009**, 24 (6), 1106–1112.
(48) Shell. http://www.shell.ca/en/aboutshell/our-business-tpkg/upstream/oil-sands/quest/technology.html. Accessed 2015.
(49) Olateju, B.; Kumar, A. Techno-economic assessment of hydrogen production from underground coal gasification (UCG) in Western Canada with carbon capture and sequestration (CCS) for upgrading bitumen from oil sands. Applied Energy **2013**, 111, 428–440.
(50) Shevalier, M.; Dalkhaa, C.; Humez, P.; Mayer, B.; Becker, V.; Nightingale, M.; Rock, L.; Zhang, G. Coupling of TOUGHREACT-Geochemist Workbench (GWB) for Modeling Changes in the Isotopic Composition of $CO_2$ Leaking from a CCS Storage Reservoir. Energy Procedia **2014**, 63, 3751–3760.
(51) Mayer, B.; Shevalier, M.; Nightingale, M.; Kwon, J.-S.; Johnson, G.; Raistrick, M.; Hutcheon, I.; Perkins, E. Tracing the movement and the fate of injected $CO_2$ at the IEA GHG Weyburn-Midale CO2 Monitoring and Storage project (Saskatchewan, Canada) using carbon isotope ratios. International Journal of Greenhouse Gas Control **2013**, 16, S177–S184.
(52) Harrington, G. J.; Clechenko, E. R.; Clay Kelly, D. Palynology and organic-carbon isotope ratios across a terrestrial Palaeocene/Eocene boundary section in the Williston Basin, North Dakota, USA. Palaeogeography, Palaeoclimatology, Palaeoecology **2005**, 226 (3–4), 214–232.
(53) Koçar, G.; Civaş, N. An overview of biofuels from energy crops: Current status and future prospects. Renewable and Sustainable Energy Reviews **2013**, 28, 900–916.
(54) Sannigrahi, P.; Ragauskas, A. J.; Tuskan, G. A. Poplar as a feedstock for biofuels: A review of compositional characteristics. Biofuels, Bioproducts and Biorefining **2010**, 4 (2), 209–226.
(55) Xu, Y.; Isom, L.; Hanna, M. A. Adding value to carbon dioxide from ethanol fermentations. Bioresource Technology **2010**, 101 (10), 3311–3319.
(56) Rossmann, A.; Butzenlechner, M.; Schmidt, H.-L. Evidence for a Nonstatistical Carbon Isotope Distribution in Natural Glucose. PLANT PHYSIOLOGY **1991**, 96 (2), 609–614.
(57) Hobbie, E. A.; Werner, R. A. Intramolecular, compound-specific, and bulk carbon isotope patterns in $C_3$ and $C_4$ plants: a review and synthesis. New Phytologist **2004**, 161 (2), 371–385.
(58) Scrimgeour, C. M.; Bennet, W. M.; Connacher, A. A. A convenient method of screening glucose for13C:12C ratio for use in stable isotope tracer studies. Biological Mass Spectrometry **1988**, 17 (4), 265–266.
(59) Weber, D.; Kexel, H.; Schmidt, H.-L. $^{13}$C-Pattern of Natural Glycerol: Origin and Practical Importance. Journal of Agricultural and Food Chemistry **1997**, 45 (6), 2042–2046.
(60) Cabañero, A. I.; Rupérez, M. Carbon isotopic characterization of cider $CO_2$ by isotope ratio mass spectrometry: a tool for quality and authenticity assessment: Carbon isotopic characterization of cider $CO_2$ by IRMS. Rapid Communications in Mass Spectrometry **2012**, 26 (16), 1753–1760.
(61) Ghoshal, S.; Zeman, F. Carbon dioxide ($CO_2$) capture and storage technology in the cement and concrete industry. In Developments and Innovation in Carbon Dioxide ($CO_2$) Capture and Storage Technology; Elsevier, 2010; pp 469–491.

(62) Srivastava, R. K.; Vijay, S.; Torres, E. Reduction of Multi-pollutant Emissions from Industrial Sectors: The U.S. Cement Industry – A Case Study. In Global Climate Change - The Technology Challenge; Princiotta, F., Ed.; Springer Netherlands: Dordrecht, 2011; Vol. 38, pp 241–272.
(63) Andres, R. J.; Marland, G.; Boden, T.; Bischof, S. Carbon dioxide emissions from fossil fuel consumption and cement manufacture, 1751–1991 and an estimate of their isotopic composition and latitudinal distribution. In The Carbon Cycle; Wigley, T. M., Schimel, D. S., Eds.; Cambridge University Press, 1994.
(64) Andres, R. J.; Marland, G.; Boden, T.; Bischof, S. Carbon Dioxide Emissions from Fossil Fuel Consumption and Cement Manufacture, 1751–1991, and an Estimate of Their Isotopic Composition and Latitudinal Distribution. In The Carbon Cycle; Wigley, T. M. L., Schimel, D. S., Eds.; Cambridge University Press: Cambridge, 2000; pp 53–62.
(65) Birat, J.-P. Carbon dioxide ($CO_2$) capture and storage technology in the iron and steel industry. In Developments and Innovation in Carbon Dioxide (Co2) Capture and Storage Technology; Elsevier, 2010; pp 492–521.
(66) Lee, A. S.; Eslick, J. C.; Miller, D. C.; Kitchin, J. R. Comparisons of amine solvents for post-combustion $CO_2$ capture: A multi-objective analysis approach. International Journal of Greenhouse Gas Control **2013**, 18, 68–74.
(67) Mook, W. G.; Bommerson, J. C.; Staverman, W. H. Carbon isotope fractionation between dissolved bicarbonate and gaseous carbon dioxide. Earth and Planetary Science Letters **1974**, 22 (2), 169–176.
(68) Tipton, P. A.; Cleland, W. W. Carbon-13 isotope effects on reactions involving carbamate and carbamoyl phosphate. Archives of Biochemistry and Biophysics **1988**, 260 (1), 273–276.
(69) Usdowski, E.; Hoefs, J. $^{13}C/^{12}C$ fractionation during the chemical absorption of $CO_2$ gas by the $NH_3$—$NH_4Cl$ buffer. Chemical Geology: Isotope Geoscience section **1988**, 73 (1), 79–85.
(70) Penn West Energy Trust. Pembina Cardium “A” Lease - $CO_2$ Pilot Project Annual Report; 2006.
(71) Sheng, X.; Nakai, S. ’ichi; Wakita, H.; Yongchang, X.; Wang, X. Carbon isotopes of hydrocarbons and carbon dioxide in natural gases in China. Journal of Asian Earth Sciences **1997**, 15 (1), 89–101.
(72) Abbas, Z.; Mezher, T.; Abu-Zahra, M. R. M. $CO_2$ purification. Part I: Purification requirement review and the selection of impurities deep removal technologies. International Journal of Greenhouse Gas Control **2013**, 16, 324–334.
(73) Chen, W.-H.; Chen, S.-M.; Hung, C.-I. Carbon dioxide capture by single droplet using Selexol, Rectisol and water as absorbents: A theoretical approach. Applied Energy **2013**, 111, 731–741.
(74) Abrosimov, V. K.; Ivanov, E. V.; Lebedeva, E. Y. Solubility and Thermodynamics of Solvation of Krypton in Aqueous-Methanol Solutions of Urea at 101325 Pa and 278–318 K. Russian Journal of General Chemistry **2005**, 75 (7), 1010–1016.
(75) Mainar, A. M.; Martínez-López, J. F.; Langa, E.; Pérez, E.; Pardo, J. I. Solubility of gases in fluoroorganic alcohols. Part II. Solubilities of noble gases in (water+1,1,1,3,3,3-hexafluoropropan-2-ol) at 298.15K and 101.33kPa. The Journal of Chemical Thermodynamics **2012**, 47, 376–381.
(76) McGrail, B. P.; Schaef, H. T.; Ho, A. M.; Chien, Y.-J.; Dooley, J. J.; Davidson, C. L. Potential for carbon dioxide sequestration in flood basalts: SEQUESTRATION IN FLOOD BASALTS. Journal of Geophysical Research: Solid Earth **2006**, 111 (B12), n/a-n/a.
(77) Emberley, S.; Hutcheon, I.; Shevalier, M.; Durocher, K.; Gunter, W. D.; Perkins, E. H. Geochemical monitoring of fluid-rock interaction and CO2 storage at the Weyburn $CO_2$-injection enhanced oil recovery site, Saskatchewan, Canada. Energy **2004**, 29 (9–10), 1393–1401.

(78) Myrttinen, A.; Becker, V.; Nowak, M.; Zimmer, M.; Pilz, P.; Barth, J. A. C. Analyses of pre-injection reservoir data for stable carbon isotope trend predictions in $CO_2$ monitoring: preparing for CO2 injection. Environmental Earth Sciences **2012**, 67 (2), 473–479.
(79) Myrttinen, A.; Becker, V.; van Geldern, R.; Würdemann, H.; Morozova, D.; Zimmer, M.; Taubald, H.; Blum, P.; Barth, J. A. C. Carbon and oxygen isotope indications for $CO_2$ behaviour after injection: First results from the Ketzin site (Germany). International Journal of Greenhouse Gas Control **2010**, 4 (6), 1000–1006.
(80) Gilfillan, S. M. V.; Haszeldine, R. S. Report on noble gas, carbon stable isotope and HCO3 measurements from the Kerr Quarter and surrounding area, Goodwater, Saskatchewan. In The Kerr Investigation - Final Report; Sherk, G. W., Ed.; 2011; pp 77–102.
(81) Gilfillan, S.; Haszedline, S.; Stuart, F.; Gyore, D.; Kilgallon, R.; Wilkinson, M. The application of noble gases and carbon stable isotopes in tracing the fate, migration and storage of $CO_2$. Energy Procedia **2014**, 63, 4123–4133.
(82) Gilfillan, S. M. V.; Ballentine, C. J.; Holland, G.; Blagburn, D.; Lollar, B. S.; Stevens, S.; Schoell, M.; Cassidy, M. The noble gas geochemistry of natural $CO_2$ gas reservoirs from the Colorado Plateau and Rocky Mountain provinces, USA. Geochimica et Cosmochimica Acta **2008**, 72 (4), 1174–1198.
(83) Ballentine, C. J.; O'Nions, R. K.; Oxburgh, E. R.; Horvath, F.; Deak, J. Rare gas constraints on hydrocarbon accumulation, crustal degassing and groundwater flow in the Pannonian Basin. Earth and Planetary Science Letters **1991**, 105 (1–3), 229–246.
(84) Ballentine, C. J.; O'Nions, R. K.; Coleman, M. L. A Magnus opus: Helium, neon, and argon isotopes in a North Sea oilfield. Geochimica et Cosmochimica Acta **1996**, 60 (5), 831–849.
(85) Pinti, D. L.; Marty, B. The origin of helium in deep sedimentary aquifers and the problem of dating very old groundwaters. Geological Society, London, Special Publications **1998**, 144 (1), 53–68.
(86) Torgersen, T.; Kennedy, B. M. Air-Xe enrichments in Elk Hills oil field gases: role of water in migration and storage. Earth and Planetary Science Letters **1999**, 167 (3–4), 239–253.
(87) Stern, L.; Baisden, W. T.; Amundson, R. Processes controlling the oxygen isotope ratio of soil $CO_2$: analytic and numerical modeling. Geochimica et Cosmochimica Acta **1999**, 63 (6), 799–814.
(88) Larson, T. E.; Breecker, D. O. Adsorption isotope effects for carbon dioxide from illite- and quartz-packed column experiments. Chemical Geology **2014**, 370, 58–68.
(89) Freundt, F.; Schneider, T.; Aeschbach-Hertig, W. Response of noble gas partial pressures in soil air to oxygen depletion. Chemical Geology **2013**, 339, 283–290.
(90) Ozima, M.; Podosek, F. A. Noble Gas Geochemistry, 2nd Edition.; Cambridge University Press, 2002.
(91) Warr, O.; Rochelle, C. A.; Masters, A.; Ballentine, C. J. Determining noble gas partitioning within a $CO_2$-$H_2O$ system at elevated temperatures and pressures. Geochimica et Cosmochimica Acta **2015**, 159, 112–125.
(92) Bernatowicz, T. J.; Podosek, F. A.; Honda, M.; Kramer, F. E. The atmospheric inventory of xenon and noble gases in shales: the plastic bag experiment. Journal of Geophysical Research **1984**, 89 (B6), 4597.
(93) Podosek, F. A.; Bernatowicz, T. J.; Kramer, F. E. Adsorption of xenon and krypton on shales. Geochimica et Cosmochimica Acta **1981**, 45 (12), 2401–2415.
(94) Bachu, S.; Bennion, D. B. Experimental assessment of brine and/or $CO_2$ leakage through well cements at reservoir conditions. International Journal of Greenhouse Gas Control **2009**, 3 (4), 494–501.
(95) Cohen, G.; Loisy, C.; Laveuf, C.; Le Roux, O.; Delaplace, P.; Magnier, C.; Rouchon, V.; Garcia, B.; Cerepi, A. The $CO_2$-Vadose project: Experimental study and modelling of $CO_2$ induced leakage and tracers associated in the carbonate vadose zone. International Journal of Greenhouse Gas Control **2013**, 14, 128–140.

(96) Carrigan, C. R.; Heinle, R. A.; Hudson, G. B.; Nitao, J. J.; Zucca, J. J. Trace gas emissions on geological faults as indicators of underground nuclear testing. Nature **1996**, 382 (6591), 528–531.
(97) Emberley, S.; Hutcheon, I.; Shevalier, M.; Durocher, K.; Mayer, B.; Gunter, W. D.; Perkins, E. H. Monitoring of fluid–rock interaction and $CO_2$ storage through produced fluid sampling at the Weyburn $CO_2$-injection enhanced oil recovery site, Saskatchewan, Canada. Applied Geochemistry **2005**, 20 (6), 1131–1157.
(98) Raistrick, M.; Mayer, B.; Shevalier, M.; Perez, R. J.; Hutcheon, I.; Perkins, E.; Gunter, B. Using Chemical and Isotopic Data to Quantify Ionic Trapping of Injected Carbon Dioxide in Oil Field Brines. Environmental Science & Technology **2006**, 40 (21), 6744–6749.
(99) Shevalier, M.; Nightingale, M.; Johnson, G.; Mayer, B.; Perkins, E.; Hutcheon, I. Monitoring the reservoir geochemistry of the Pembina Cardium $CO_2$ monitoring project, Drayton Valley, Alberta. Energy Procedia **2009**, 1 (1), 2095–2102.
(100) Lu, J.; Kharaka, Y. K.; Thordsen, J. J.; Horita, J.; Karamalidis, A.; Griffith, C.; Hakala, J. A.; Ambats, G.; Cole, D. R.; Phelps, T. J.; et al. $CO_2$–rock–brine interactions in Lower Tuscaloosa Formation at Cranfield $CO_2$ sequestration site, Mississippi, U.S.A. Chemical Geology **2012**, 291, 269–277.
(101) Györe, D.; Stuart, F. M.; Gilfillan, S. M. V.; Waldron, S. Tracing injected $CO_2$ in the Cranfield enhanced oil recovery field (MS, USA) using He, Ne and Ar isotopes. International Journal of Greenhouse Gas Control **2015**, 42, 554–561.
(102) Gilfillan, S. M. V.; Lollar, B. S.; Holland, G.; Blagburn, D.; Stevens, S.; Schoell, M.; Cassidy, M.; Ding, Z.; Zhou, Z.; Lacrampe-Couloume, G.; et al. Solubility trapping in formation water as dominant CO2 sink in natural gas fields. Nature **2009**, 458 (7238), 614–618.
(103) Clark-Thorne, S. T.; Yapp, C. J. Stable carbon isotope constraints on mixing and mass balance of $CO_2$ in an urban atmosphere: Dallas metropolitan area, Texas, USA. Applied Geochemistry **2003**, 18 (1), 75–95.
(104) Pataki, D. E.; Ehleringer, J. R.; Flanagan, L. B.; Yakir, D.; Bowling, D. R.; Still, C. J.; Buchmann, N.; Kaplan, J. O.; Berry, J. A. The application and interpretation of Keeling plots in terrestrial carbon cycle research: APPLICATION OF KEELING PLOTS. Global Biogeochemical Cycles **2003**, 17 (1), n/a-n/a.
(105) Porcelli, D.; Ballentine, C. J.; Wieler, R. An Overview of Noble Gas Geochemistry and Cosmochemistry. Reviews in Mineralogy and Geochemistry **2002**, 47 (1), 1–19.
(106) Lee, J.-Y.; Marti, K.; Severinghaus, J. P.; Kawamura, K.; Yoo, H.-S.; Lee, J. B.; Kim, J. S. A redetermination of the isotopic abundances of atmospheric Ar. Geochimica et Cosmochimica Acta **2006**, 70 (17), 4507–4512.
(107) Amundson, R.; Stern, L.; Baisden, T.; Wang, Y. The isotopic composition of soil and soil-respired $CO_2$. Geoderma **1998**, 82 (1–3), 83–114.
(108) Romanak, K. D.; Bennett, P. C.; Yang, C.; Hovorka, S. D. Process-based approach to $CO_2$ leakage detection by vadose zone gas monitoring at geologic $CO_2$ storage sites: PROCESS-BASED LEAKAGE DETECTION. Geophysical Research Letters **2012**, 39 (15), n/a-n/a.
(109) Klump, S.; Tomonaga, Y.; Kienzler, P.; Kinzelbach, W.; Baumann, T.; Imboden, D. M.; Kipfer, R. Field experiments yield new insights into gas exchange and excess air formation in natural porous media. Geochimica et Cosmochimica Acta **2007**, 71 (6), 1385–1397.
(110) Romanak, K. D.; Wolaver, B.; Yang, C.; Sherk, G. W.; Dale, J.; Dobeck, L. M.; Spangler, L. H. Process-based soil gas leakage assessment at the Kerr Farm: Comparison of results to leakage proxies at ZERT and Mt. Etna. International Journal of Greenhouse Gas Control **2014**, 30, 42–57.
(111) Gal, F.; Michel, K.; Pokryszka, Z.; Lafortune, S.; Garcia, B.; Rouchon, V.; de Donato, P.; Pironon, J.; Barres, O.; Taquet, N.; et al. Study of the environmental variability of gaseous emanations over a $CO_2$ injection pilot—Application to the French Pyrenean foreland. International Journal of Greenhouse Gas Control **2014**, 21, 177–190.

(112) Schacht, U.; Jenkins, C. Soil gas monitoring of the Otway Project demonstration site in SE Victoria, Australia. International Journal of Greenhouse Gas Control **2014**, 24, 14–29.
(113) Schacht, U.; Regan, M.; Boreham, C.; Sharma, S. $CO_2$CRC Otway project–Soil gas baseline and assurance monitoring 2007–2010. Energy Procedia **2011**, 4, 3346–3353.
(114) Carroll, S.; Hao, Y.; Aines, R. Geochemical detection of carbon dioxide in dilute aquifers. Geochemical Transactions **2009**, 10 (1), 4.
(115) Grossman, E. L.; Coffman, B. K.; Fritz, S. J.; Wada, H. Bacterial production of methane and its influence on ground-water chemistry in east-central Texas aquifers. Geology **1989**, 17 (6), 495.
(116) Hellings, L.; Van den Driessche, K.; Baeyens, W.; Keppens, E.; Dehairs, F. Origin and fate of dissolved inorganic carbon in interstitial waters of two freshwater intertidal areas: A case study of the Scheldt Estuary, Belgium. Biogeochemistry **2000**, 51 (2), 141–160.
(117) Sharma, S.; Frost, C. D. Tracing Coalbed Natural Gas–Coproduced Water Using Stable Isotopes of Carbon. Ground Water **2008**, 46 (2), 329–334.
(118) Simpkins, W. W.; Parkin, T. B. Hydrogeology and redox geochemistry of $CH_4$ in a Late Wisconsinan Till and Loess Sequence in central Iowa. Water Resources Research **1993**, 29 (11), 3643–3657.
(119) Mackintosh, S. J.; Ballentine, C. J. Using $^3He/^4He$ isotope ratios to identify the source of deep reservoir contributions to shallow fluids and soil gas. Chemical Geology **2012**, 304–305, 142–150.
(120) Hendry, J. M.; Schwartz, F. W.; Robertson, C. Hydrogeology and hydrochemistry of the Milk River aquifer system, Alberta, Canada: a review. Applied Geochemistry **1991**, 6 (4), 369–380.
(121) Andrews, J. N.; Drimmie, R. J.; Loosli, H. H.; Hendry, M. J. Dissolved gases in the Milk River aquifer, Alberta, Canada. Applied Geochemistry **1991**, 6 (4), 393–403.
(122) Klusman, R. W. Rate measurements and detection of gas microseepage to the atmosphere from an enhanced oil recovery/sequestration project, Rangely, Colorado, USA. Applied Geochemistry **2003**, 18 (12), 1825–1838.
(123) Sherk, G. W.; Romanak, K. D.; Dale, J.; Gilfillan, S. M. V.; Haszeldine, R. S.; Ringler, E. S.; Wolaver, B. D.; Yang, C. The Kerr Investigation: Final Report. Findings ofr the investigation into the impact of CO2 on the Kerr Property; IPAC-CO2 Research Inc., 2011.
(124) Romanak, K. D.; Changbing, Y. Analysis of gas geochemistry at the Kerr Site. In The Kerr Investigation - Final Report; Sherk, G. W., Ed.; 2011; pp 57–76.
(125) Krevor, S.; Perrin, J.-C.; Esposito, A.; Rella, C.; Benson, S. Rapid detection and characterization of surface $CO_2$ leakage through the real-time measurement of δ13δ13 C signatures in $CO_2$ flux from the ground. International Journal of Greenhouse Gas Control **2010**, 4 (5), 811–815.
(126) McAlexander, I.; Rau, G. H.; Liem, J.; Owano, T.; Fellers, R.; Baer, D.; Gupta, M. Deployment of a Carbon Isotope Ratiometer for the Monitoring of $CO_2$ Sequestration Leakage. Analytical Chemistry **2011**, 83 (16), 6223–6229.
(127) Spangler, L. H.; Dobeck, L. M.; Repasky, K. S.; Nehrir, A. R.; Humphries, S. D.; Barr, J. L.; Keith, C. J.; Shaw, J. A.; Rouse, J. H.; Cunningham, A. B.; et al. A shallow subsurface controlled release facility in Bozeman, Montana, USA, for testing near surface $CO_2$ detection techniques and transport models. Environmental Earth Sciences **2010**, 60 (2), 227–239.
(128) Blackford, J.; Stahl, H.; Bull, J. M.; Bergès, B. J. P.; Cevatoglu, M.; Lichtschlag, A.; Connelly, D.; James, R. H.; Kita, J.; Long, D.; et al. Detection and impacts of leakage from sub-seafloor deep geological carbon dioxide storage. Nature Climate Change **2014**, 4 (11), 1011–1016.
(129) Gilfillan, S. M. V.; Wilkinson, M.; Haszeldine, R. S.; Shipton, Z. K.; Nelson, S. T.; Poreda, R. J. He and Ne as tracers of natural $CO_2$ migration up a fault from a deep reservoir. International Journal of Greenhouse Gas Control **2011**, 5 (6), 1507–1516.

(130) Prinzhofer, A.; Dos Santos Neto, E. V.; Battani, A. Coupled use of carbon isotopes and noble gas isotopes in the Potiguar basin (Brazil): Fluids migration and mantle influence. Marine and Petroleum Geology **2010**, 27 (6), 1273–1284.
(131) Kotarba, M. J.; Nagao, K.; Karnkowski, P. H. Origin of gaseous hydrocarbons, noble gases, carbon dioxide and nitrogen in Carboniferous and Permian strata of the distal part of the Polish Basin: Geological and isotopic approach. Chemical Geology **2014**, 383, 164–179.

## Tables

**Table 1. Summary of Noble Gas concentrations and solubilities**

| | Air (ppbv)[a] | Water (ppbv)[b] | Oil (mol ppb) | Gas (mol ppb) | Solubility in water[g] | Solubility in oil[g] |
|---|---|---|---|---|---|---|
| $^{4}He$ | 5,240 | 50 | 12,000 to 130,000[c] | 580 to 3,838,000[e,f] | 0.0090 | 0.0211 |
| $^{20}Ne$ | 18,180 | 181 | 2 to 21[c] | 4.1 to 1,294.4[e,f] | 0.0096 | 0.0198 |
| $^{40}Ar$ | 9,340,000 | 398,400 | 10,700 to 26,900[c] | 51,100 to 208,300[6] | 0.036 | 0.0158 |
| $^{36}Ar$ | 31,607 | 1,348 | 1 to 151[d] | 20 to 11,849[e,f] | | |
| $^{84}Kr$ | 650 | 51 | | 1.6 to 120[e,f] | 0.0388 | 0.400 |
| $^{136}Xe$ | 8 | 0.9 | | 0.1 to 5.7[e,f] | 0.0603 | 1.080 |

*[a] Calculated from Porcelli et al. (2002)[105]. [b] Based on calculated equilibrium concentrations of elemental noble gases in low salinity water at 10 °C from Lake Baikal[32], using the simplified assumption that 1 g of water = 1 $cm^3$, and converted to isotopic abundances using isotopic ratios from Porcelli et al. (2002)[105]. [c] Calculated from Ballentine et al (1996)[85]; [d] Calculated from Torgersen and Kennedy (1999)[87]; [e] calculated from Prinzhofer et al (2010)[130]; [f] calculated from Kotarba et al (2014)[131]; [g] Solubilities[130] expressed as the ratio of the noble gas concentration in the liquid to the concentration in the gas (mol $m^{-3}$ / mol $m^{-3}$), at 50 °C and atmospheric pressure for water and heavy (API 25) oil.*

**Table 2. Expected C-isotope and noble gas compositions of the $CO_2$ stream generated by a variety of industrial and energy generating technologies, relative to their source components (feedstock, combustion atmosphere etc.) and with likely fractionations where relevant.** Subsequent amine capture or physical absorption are not included. For processes that will be followed with amine capture (* in "Process" column), add: $\delta^{13}C$ enrichment of -20 to +2.5 ‰, and depletion of noble gas concentrations (especially light noble gases). For physical absorption in organic solvents (may or may not be used with all other processes), add a small positive C-isotopic enrichment, dependent on the relative efficiencies of the absorption and desorption processes, and depletion of noble gas concentrations (especially light noble gases). References for the C-isotope composition of feedstock and other components are given in the text and in the supplementary data tables, and values are summarised in Figure 1.

| Process | Feedstock | $\delta^{13}C$ ‰ V-PDB of feedstock | $\delta^{13}C$ Ɛ ‰ of process | $\delta^{13}C$ of $CO_2$ ‰ V-PDB | Noble gas content of components | Noble Gases in $CO_2$ |
|---|---|---|---|---|---|---|
| Normal Combustion * | Coal | -30 to -20 | -1.3 | -31.3 to -21.3 | High $^4He$ and $^{40}Ar$ in fossil fuels. Atmospheric noble gases from air. | Air-like, plus enriched $^4He$ and $^{40}Ar$. |
| | Oil | -36 to -18 | | -37.3 to -19.3 | | |
| | Natural Gas | <-60 to -20 | | <-61 to -21.3 | | |
| | C3 biomass | -30 to -24 | 0 | -30 to -24 | Atmospheric noble gases | Air-like noble gases |
| | C4 biomass | -15 to -10 | 0 to +4 | -15 to -6 | | |
| Oxyfuel | Coal | -30 to -20 | -1.3 | -31.3 to -21.3 | High $^4He$ and $^{40}Ar$ in fossil fuels. Heavy noble gases in cryogenic oxygen. | Enriched in heavy noble gases, $^4He$ and $^{40}Ar$. |
| | Oil | -36 to -18 | -1.3 | -37.3 to -19.3 | | |
| | Natural Gas | <-60 to -20 | -1.3 | <-61 to -21.3 | | |
| | C3 biomass | -30 to -24 | 0 | -30 to -24 | Heavy noble gases in cryogenic oxygen. | Enriched in heavy noble gases. |
| | C4 biomass | -15 to -10 | 0 to +4 | -15 to -6 | | |
| Gasification / Syngas | Coal | -30 to -20 | Difficult to predict. Possible small –ve Ɛ | <-30 to <-20 | High $^4He$ and $^{40}Ar$ in fossil fuels. Use of steam will add atmospheric noble gases. Use of cryogenic $O_2$ will add heavy noble gases. | Atmospheric noble gases. Possibly enriched in heavy noble gases. High $^4He$ and $^{40}Ar$ for fossil fuel feedstocks. |
| | Oil | -36 to -18 | | <-36 to < -18 | | |
| | Natural Gas | <-60 to -20 | | <-60 to < -20 | | |
| | C3 biomass | -30 to -24 | | <-30 to <-24 | | |
| | C4 biomass | -15 to -10 | | <-15 to <-10 | | |
| Synfuel / chemical plant | Coal | -30 to -20 | Possible small +ve Ɛ | >-30 to >-20 | Increased likelihood of using cryogenic $O_2$ will add heavy noble gases | Air like ratios and likely enriched in heavy noble gases |
| | Oil | -36 to -18 | | >-36 to > -18 | | |
| | Natural Gas | <-60 to -20 | | >-60 to > -20 | | |
| Fermentation | C4 Sugars | -15 to -10 | +4 to +6 | -11 to -4 | Air saturated water | Air-like ratios, depleted concentrations relative to air. |
| Cement * | Coal + Limestone | -30 to -20<br>0 | -1.3 for coal + mixing | -16 to -11 | High $^4He$ and $^{40}Ar$ in fossil fuels. Atmospheric noble gases from air. Heavy noble gas enrichment for oxyfuel. | Air-like, plus enriched $^4He$ and $^{40}Ar$. Heavy noble gas enrichment for oxyfuel. |
| Steel Industry: ISP * | Coal | -30 to -20 | -1.3 | -31.3 to -21.3 | High $^4He$ and $^{40}Ar$ in fossil fuels. Atmospheric noble gases from air. | Air-like, plus enriched $^4He$ and $^{40}Ar$. |
| Steel Industry: DRI | As for Syngas Iron ore | As for Syngas | | | High $^4He$ and $^{40}Ar$ in iron oxide. Atmospheric noble gases from air. Heavy noble gases in cryogenic oxygen? | Air-like, plus enriched $^4He$ and $^{40}Ar$. Possibly enriched in heavy noble gases. |
| Natural gas processing (Amine capture) | $CO_2$ co-existing with natural gas | -14 to +14 | -20 to +2.5 | -34 to +21 | High $^4He$ and $^{40}Ar$ in natural gas. | Noble gases likely lost during capture. Preferential retention of heavy noble gases. Radiogenic and terrigenic isotope ratios retained but abundances << air. |

## Figures

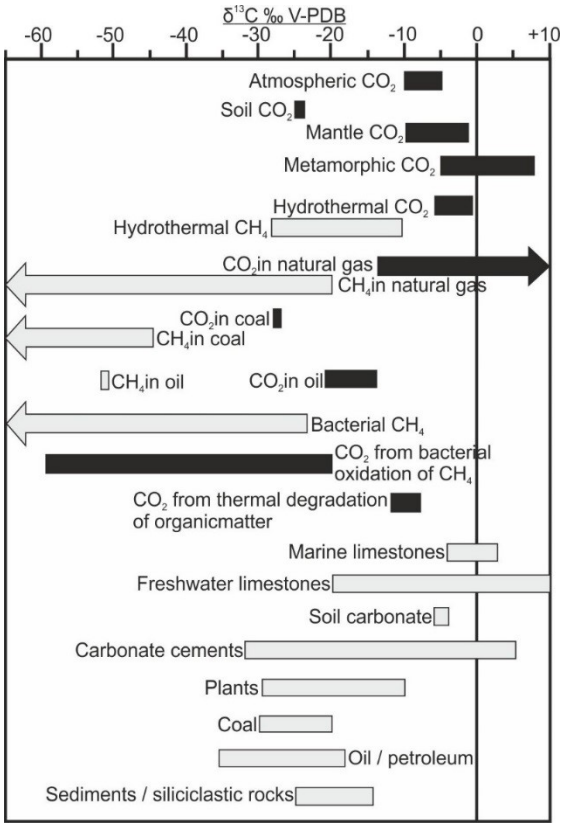


**Figure 1. C-isotope values for a range of naturally occurring materials. Black boxes indicate $CO_2$. Grey boxes are other substances. Arrows represent values off the scale of the diagram. See Supplementary data Table S1 for references. Note that a wide range of $\delta^{13}C$ values are covered by naturally occurring $CO_2$ sources.**

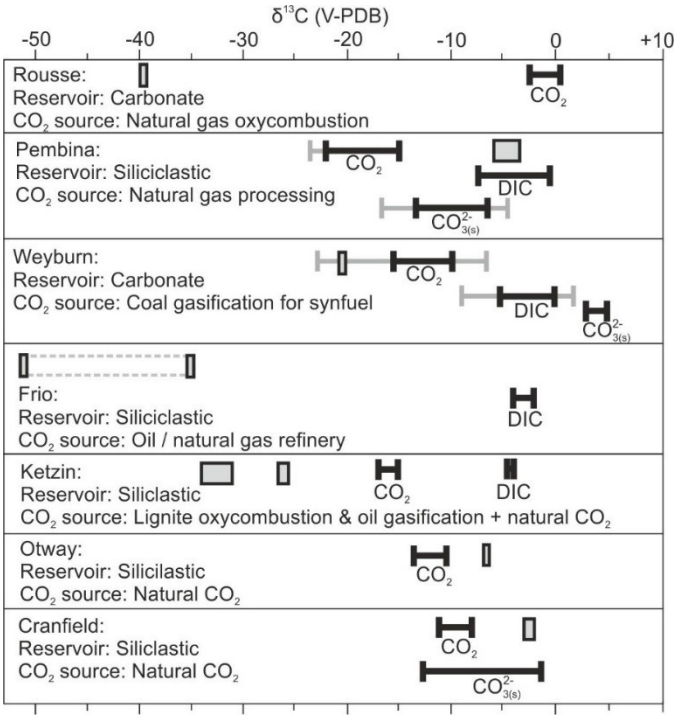


**Figure 2: Comparison of injected $CO_2$ $\delta^{13}C$ values with reservoir baseline $CO_2$, DIC and carbonate minerals in existing CCS projects. Grey boxes show the $\delta^{13}C$ of injected $CO_2$; Frio and Ketzin show 2 boxes each to reflect the two anthropogenic $CO_2$ sources used in these projects. Reservoir baseline values for $CO_2$, DIC and carbonate minerals are shown by horizontal crosshair lines. Where the baseline data are variable, the full range in values is shown by grey lines while the majority of data are represented by black lines. See Tables S2-S4 for references.**

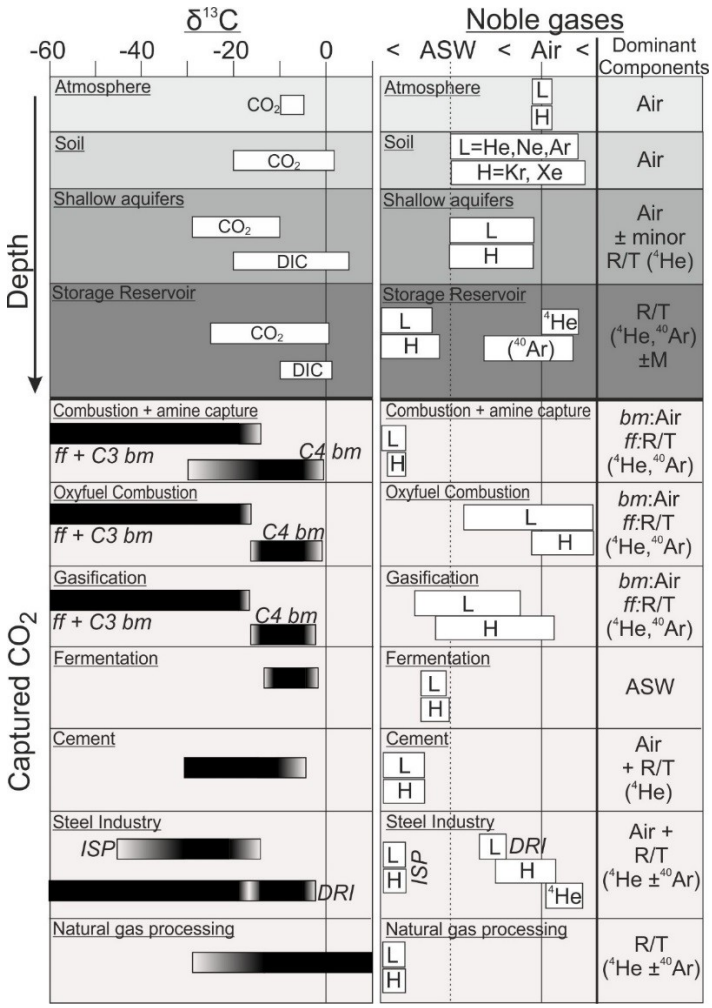


**Figure 3. Comparison of the range of inherent tracer values for storage and leakage reservoirs (Tables S1-S6), and the expected captured $CO_2$ composition for various $CO_2$ sources (Table 2). Boxes represent the range of $\delta^{13}C$ (V-PDB) and noble gas concentration (relative to air and ASW) in baseline conditions for atmosphere, soil, shallow aquifers and storage reservoirs, compared to the range of values expected for different sources of captured $CO_2$. C-isotopes are given in δ notation relative to V-PDB. Noble gases shown for absolute concentrations relative to air and ASW, with dominant components resolvable by isotopic analysis; "L" = light noble gases, "H" = heavy noble gases, "R/T" = radiogenic and / or terrigenic component, "M" = mantle component, "ASW" = air saturated water. *ff* = fossil fuels; *bm* = biomass; *ISP* = integrated steel plant; *DRI* = directly reduced iron.**